Supporting Information

Porphyrin Bearing Phenothiazine Pincers as Hosts for Fullerene Binding via Concave-Convex Complementarity: Synthesis and Complexation Study

Kanika Jain,[a] Naresh Duvva,[b] Tapta Kanchan Roy,*[c] Lingamallu Giribabu.*[bd] and Raghu Chitta,*[ae]

[a]*Department of Chemistry, School of Chemical Sciences & Pharmacy, Central University of Rajasthan, Kishangarh, Dist. Ajmer, Rajasthan-305817, India.*

[b]*Polymers and Functional Materials Division, CSIR-Indian Institute of Chemical Technology, Tarnaka, Hyderabad-500007, Telangana, India.*

[c]*Department of Chemistry and Chemical Sciences, Central University of Jammu, Rahya-Suchani (Bagla), Dist: Samba, Jammu and Kashmir 181143, India*

[d]*Academy of Scientific and Innovative Research, Ghazianbad 201002, India*

[e]*Department of Chemistry, National Institute of Technology Warangal, Hanamkonda, Dist: Hanamkonda, Telangana 506004, India.*

Supporting Information

Supporting Information

Supporting Information

1. Experimental Section

1.1 Synthesis Details

10-(2-bromoethyl)-10H-phenothiazine (1):[1] Sodium hydride (60% mineral oil, 1.2 g, 50.2 mmol) was taken in DMF and to this, a solution of phenothiazine (5 g, 0.025 mol) in DMF was added at 0˚C under nitrogen while stirring. The reaction mixture was stirred at 0˚C for 30 min. and raised to RT and stirred for 1 h under nitrogen. The reaction was again cooled to 0°C, 1,2-dibromoethane (47 g, 0.25 mol) was added and the reaction mixture was stirred at 90°C for 12 h under nitrogen. The reaction mixture was cooled to room temperature, washed with water, and extracted with ethyl acetate. The organic phase was washed with brine solution, dried over Na_2SO_4 and filtered. The crude mixture was purified using silica gel column chromatography and the desired compound was obtained using petroleum ether: ethyl acetate (20:1, v/v) as the eluent. Evaporation of the solvent under reduced pressure yielded the titled compound as a white solid. Yield: 3.8 g (49%). ^{1}H NMR (500 MHz, $CDCl_3$): δ (in ppm): 7.20-7.15 (m, 4H, *phenothiazine-aromatic H*), 6.96 (t, 2H, *J* = 10 Hz, *phenothiazine-aromatic H*), 6.84 (d, 2H, *J* = 12 Hz, *phenothiazine-aromatic H*), 4.29 (t, 2H, *J* = 10 Hz, *Br-CH*$_2$), 3.64 (t, 2H, *J* = 9.5 Hz, *N-CH*$_2$). HRMS (ESI) (m/z): [M^+] Calcd for $C_{14}H_{12}BrNS$: 306.22; found: 306.2210.

4-(2-(10*H*-phenothiazin-10-yl)ethoxy)benzaldehyde (2b):[1] To a solution of 4-hydroxy benzaldehyde (0.1 g, 0.8 mmol) in DMF (50 mL), dry potassium carbonate (0.9 g, 6.5 mmol) was added and stirred under argon for 30 min. Then **1** (0.5 g, 1.6 mmol) was added and the reaction mixture was stirred at 90°C for 3 h, cooled to room temperature and the solvent was evaporated. To this concentrated crude mixture, water was added and was extracted using ethyl acetate. The organic layer was evaporated and the crude compound was purified by silica gel column chromatography using petroleum ether:ethylacetate (20:1, v/v) as an eluent. Evaporation of the solvent yielded the titled compound as a light yellow solid. Yield: 0.4 g, (71%). ^{1}H NMR (500 MHz, $CDCl_3$): δ (in ppm): 9.88 (s, 1H, *-CHO*), 7.82 (d, 2H, *J* = 8.5 Hz, *phenyl-aromatic H*), 7.17 (d, 4H, *J* = 8.0 Hz, *phenyl-aromatic 2H & phenothiazine-aromatic 2H*), 7.00-6.94 (m, 6H, *phenothiazine-aromatic H*), 4.38 (s, 4H, *O-CH*$_2$ & *N-CH*$_2$). HRMS (ESI): (m/z): [M^+] Calcd for $C_{21}H_{17}NO_2S$: 347.4320; [M+H]$^+$ found: 348.4410.

10-Hexyl-10H-phenothiazine (Hexyl-PTZ):[2] NaH (1.20 g, 30.10 mmol, 60%) was washed with petroleum ether in 250 mL round bottomed flask and petroleum ether was decanted after washing. To this phenothiazine (5.00 g, 25.09 mmol) dissolved in 120 mL of DMF was added using dropping

funnel and the mixture was stirred at room temperature under nitrogen for 1 h. Then the reaction mixture was cooled using ice and 1-bromohexane (4.97 g, 30.10 mmol) was added drop wise. The resulting reaction mixture was stirred overnight at room temperature. The progress of the reaction was monitored using TLC. Upon consumption of the limiting reagent phenothiazine the reaction mixture was quenched using ammonium chloride (0.1M, 10 mL) and ice water. The reaction mixture was then extracted using ethyl acetate. The reaction mixture was washed using brine solution and passed through sodium sulphate (Na_2SO_4). The solvent was removed under pressure on the rotary evaporator and the residue was subjected to silica gel column chromatography using petroleum ether as eluent to give the titled compound as a transparent viscous liquid (6.39 g, 90%). ^{1}H NMR (500 MHz, $CDCl_3$):δ (in ppm): 7.17- 7.13 (m, 4H, *phenothiazine-H*), 6.93- 6.86 (m, 4H, *phenothiazine-H*), 3.84 (t, 2H, *J* = 6.7Hz, -CH_2), 1.82- 1.79 (m, 2H, -CH_2), 1.32- 1.28 (m, 6H, -CH_2), 0.89- 0.88 (m, 3H, -CH_3). ESI-MS (m/z): [M^+] Calcd for $C_{18}H_{21}NS$: 283; $[M+H]^+$ found: 284.

H_2-5,10,15,20-tetraphenylporphyrin (H_2TPP): This control compound was synthesized as per the method reported in literature.[3] A solution of (1.0 g, .9.5 mmol) of benzaldehyde and (0.63 g, 9.5 mmol) of pyrrole in 100 mL of propionic acid was refluxed for an hour. The progress of the reaction was monitored using TLC and upon complete consumption of the aldehyde, propionic acid was removed by distillation under reduced pressure. The resulting solid was wash with methanol and was subjected to further purification by silica gel column chromatography. The compound was eluted using 1:1 (v/v) chloroform and pet ether.Yield: 0.87 g (16%). ^{1}H NMR (500 MHz, $CDCl_3$): (δ in ppm): 8.86 (s, 8H, *β*-pyrrole), 8.22-8.20 (m, 8H, *o*-phenyl *H*), 7.77-7.72 (m, 12H, *m* and *p*-phenyl *H*) and -2.77 (s, 2H, *NH*).

1.2 Methods and Instrumentation

1.2.1. Computational details. The molecular size of all four clusters are considerably large (total, 1186 and 1246 number of electrons) for any level of quantum chemical calculations and hence a balance between computational cost and accuracy is required to deal such systems. Here, the first-principles based viable DFT based method is used which is computationally faster yet accurate to determine molecular structures. Due to high flexibility in the molecular systems, all four types of molecules are expected to give several low energy conformers. Hence a systematic conformational analysis is performed using DFT based hybrid B3LYP[4, 5] method. In the first step, several initial pool of structures are freely optimized at B3LYP/3-21G(d) level of theory as suggested by Zandler and

D'Souza.[6] It is found that several initial guess structures with little different orientations converge to the same equilibrium structure. Next, a few such lower energy structures near the global minima were chosen from the pool of optimized structures. Considering the several weak interactions present in the four structures, Grimme's dispersion correction B3LYP-D3 with BJ-damping [7, 8] in conjunction with 3-21G(d) basis sets was applied for further optimization. It is found that dispersion corrections has a prominent effect on the determination of the structures of this type of molecules. Starting from the optimized structures obtained without dispersion corrections, different orientations following the rotations of the dihedral angels of phenothiazine moieties were found after considering dispersion corrections which apparently addressed better weak interactions. The better description offered by the dispersion corrections to the multiple non-covalent interactions with fullerene present in the systems results more reliable structures. Among all the calculated structures, the lowest energy conformers were determined for each of the four cases. Finally, to further validate the reliability of the calculated structures, higher basis 6-31G(d) in conjunction with B3LYP-D3 method were carried out and similar quality of structures were obtained for both the basis sets.

The binding energy between the phenothiazine moiety and fullerene in vacuum is defined by the formula:

$$\Delta E \text{ (binding energy)} = E \text{ (fullerene-PTZ moiety)} - [E \text{ (fullerene in vacuum)} + E \text{ (free PTZ in vacuum)}]$$

These calculations were performed considering the cluster geometries are rigid, such that when the non-covalent interactions are withdrawn, the fragments retain the same geometries that they possess in the equilibrium structure. All the calculations were performed in Gaussian 16 program suit.[9]

Supporting Information

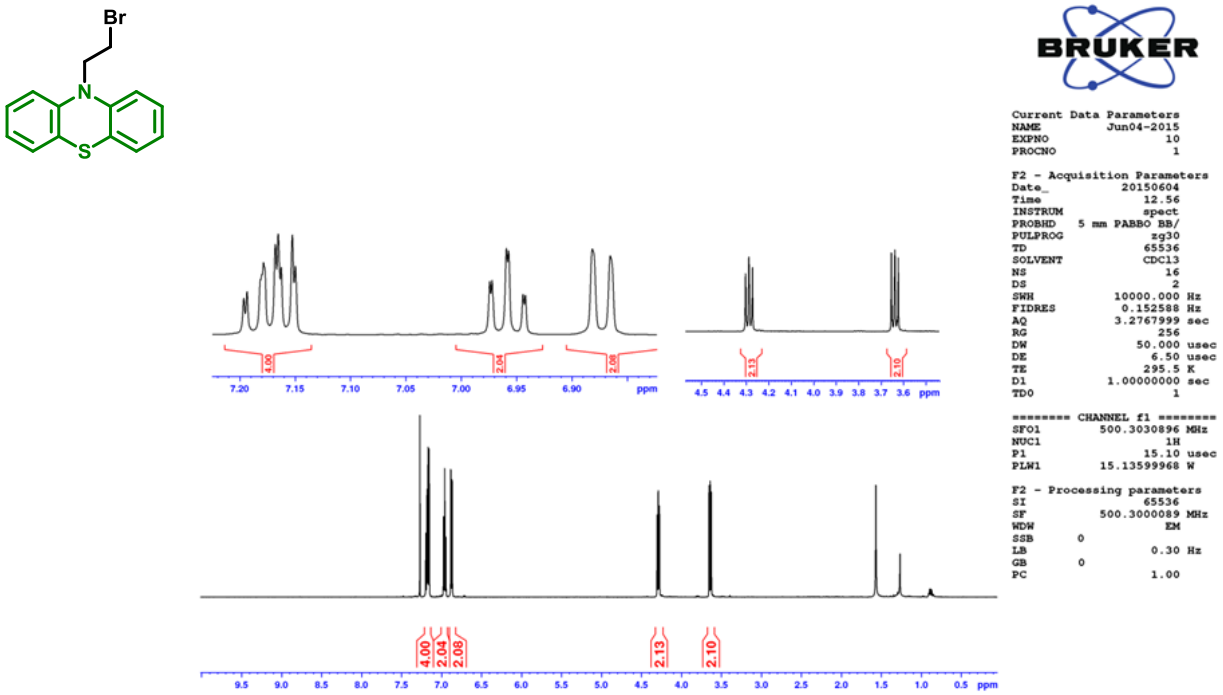

Fig.S1. ^{1}H NMR spectrum of10-(2-bromoethyl)-10H-phenothiazine **(1)** in $CDCl_3$.

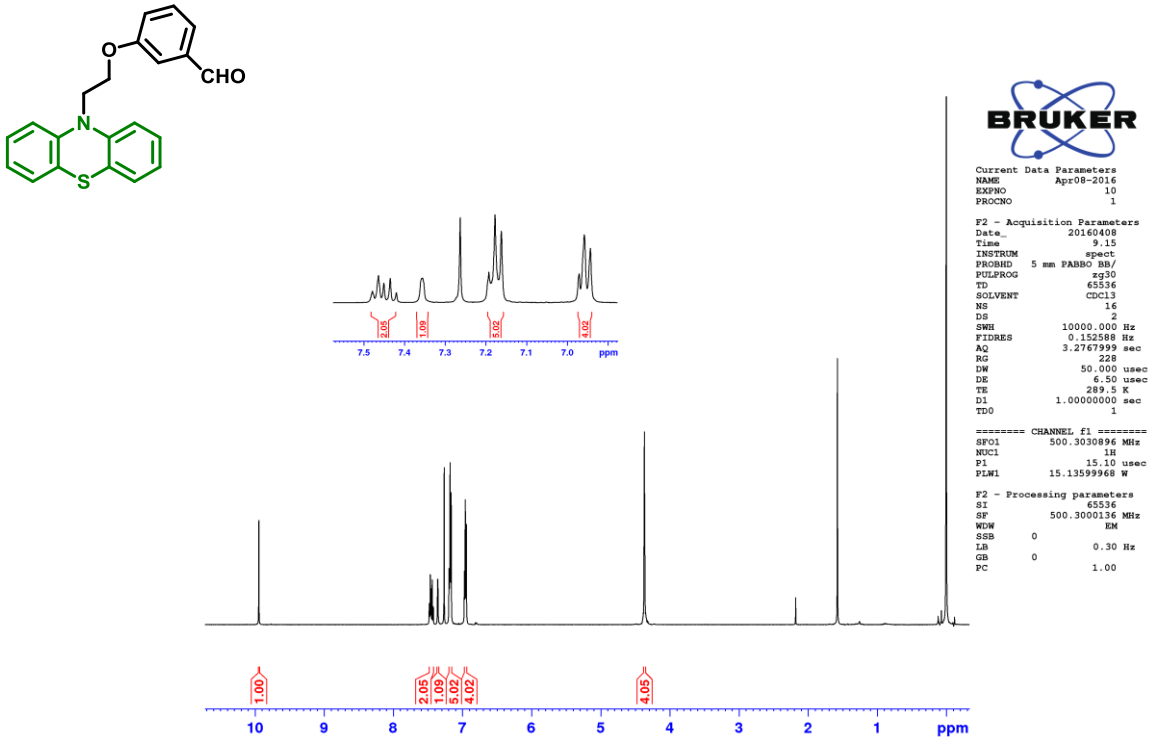

Fig. S2. ^{1}H NMR spectrum 3-(2-(10*H*-phenothiazin-10-yl)ethoxy)benzaldehyde **(2a)** in $CDCl_3$.

Supporting Information

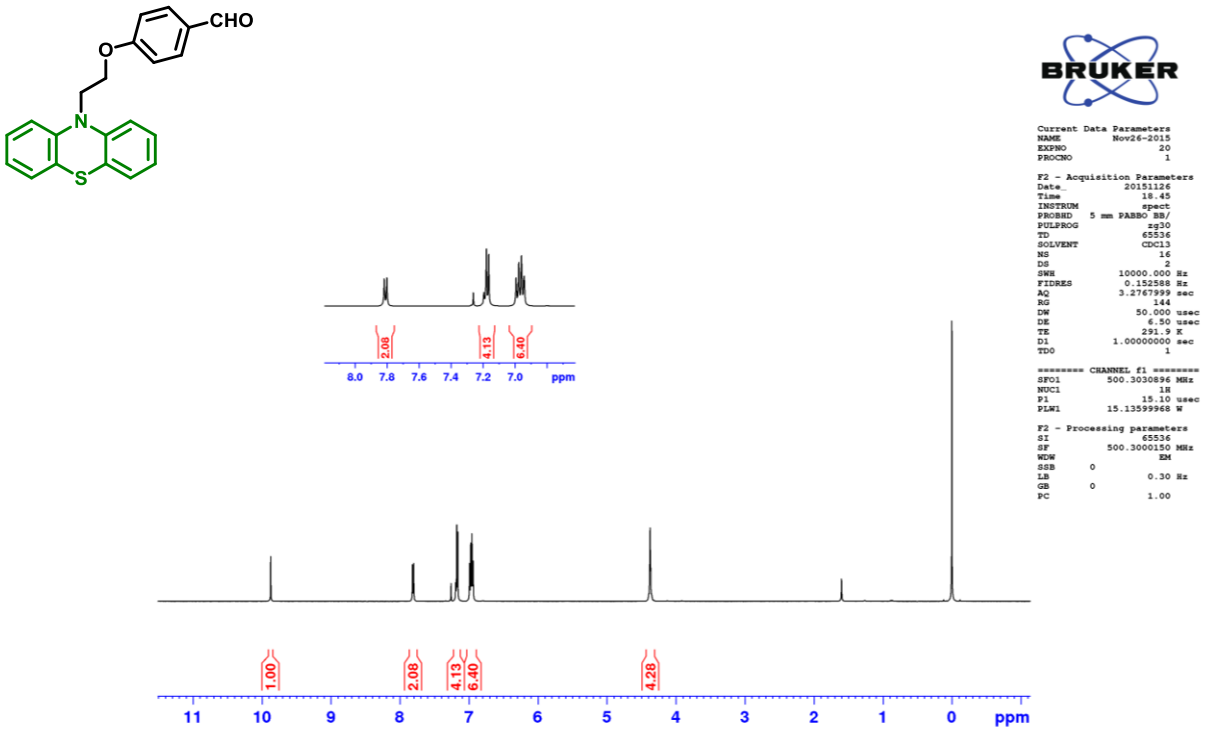

Fig.S3. ^{1}H NMR spectrum of 4-(2-(10*H*-phenothiazin-10-yl)ethoxy)benzaldehyde **(2b)** in $CDCl_3$.

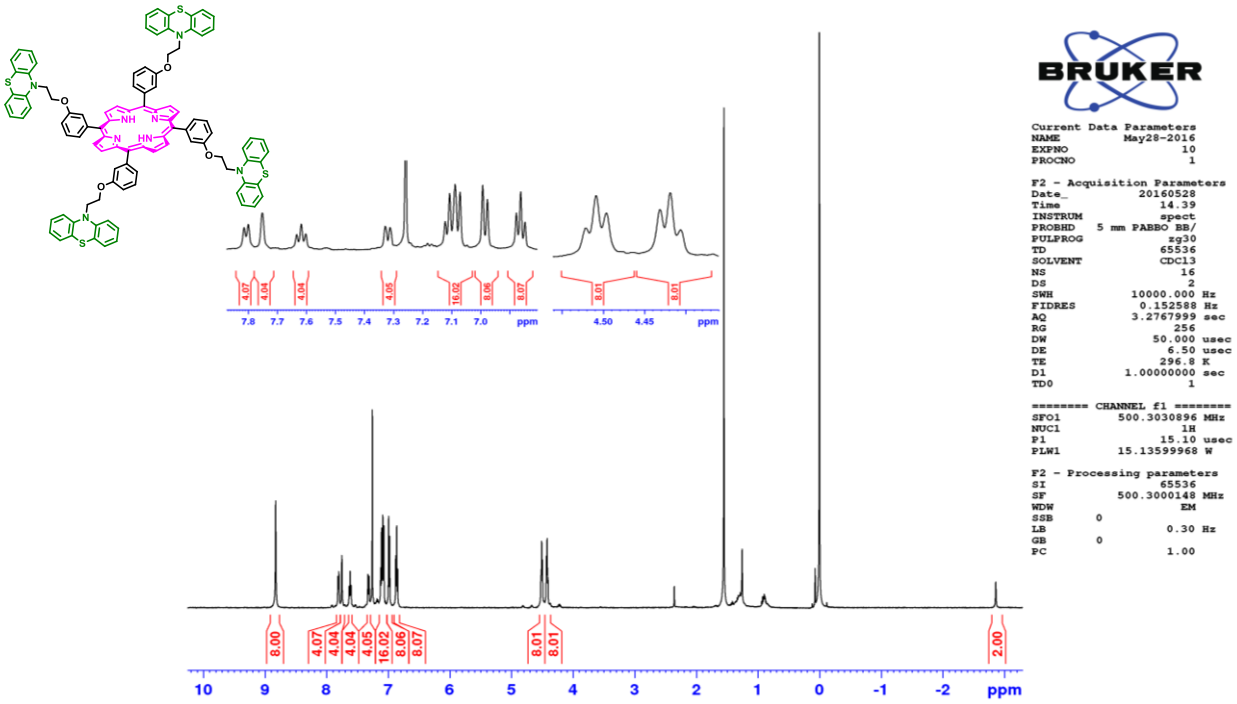

Fig.S4. ^{1}H NMR spectrum of 5, 10, 15, 20-tetra-3-(2-(10H-phenothiazin-10-yl)ethoxy) phenyl free base porphyrin, ***m*-(PTZ)$_4$-H$_2$P** in $CDCl_3$.

Supporting Information

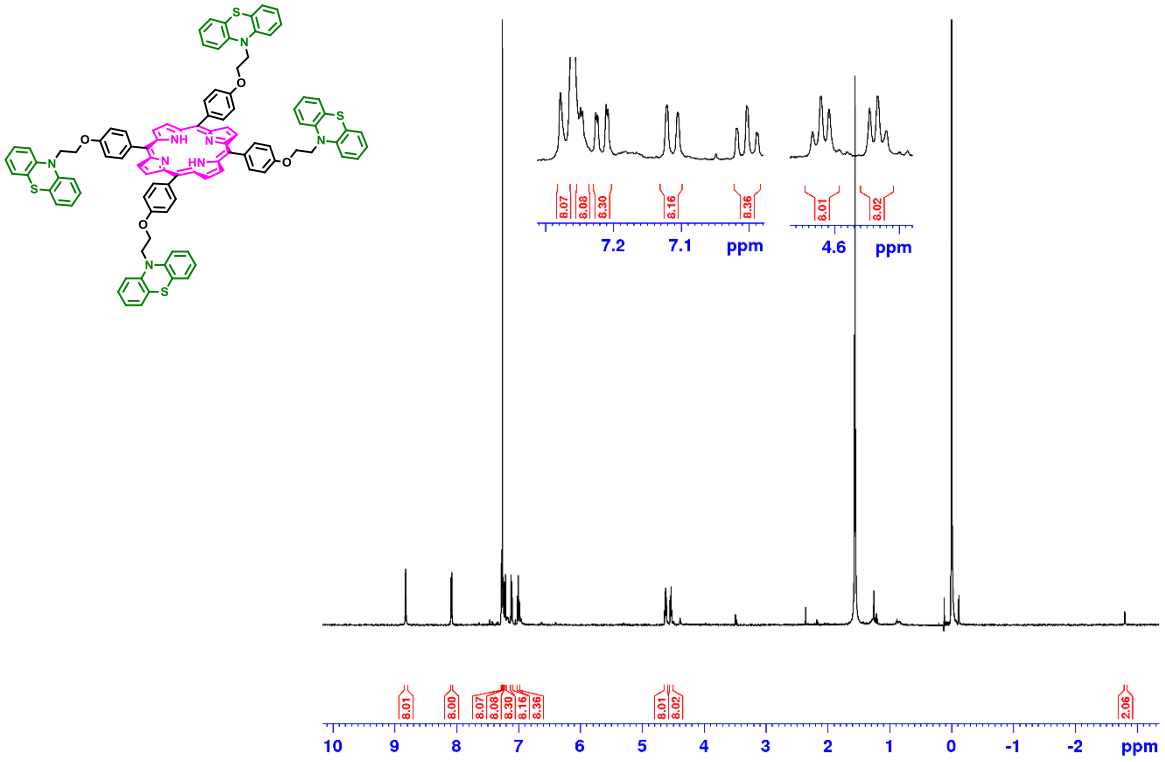

Fig.S5. ^{1}H NMR spectrum of 5, 10, 15, 20-tetra-4-(2-(10H-phenothiazin-10-yl)ethoxy) phenyl free base porphyrin, ***p*-(PTZ)$_4$-H$_2$P** in $CDCl_3$.

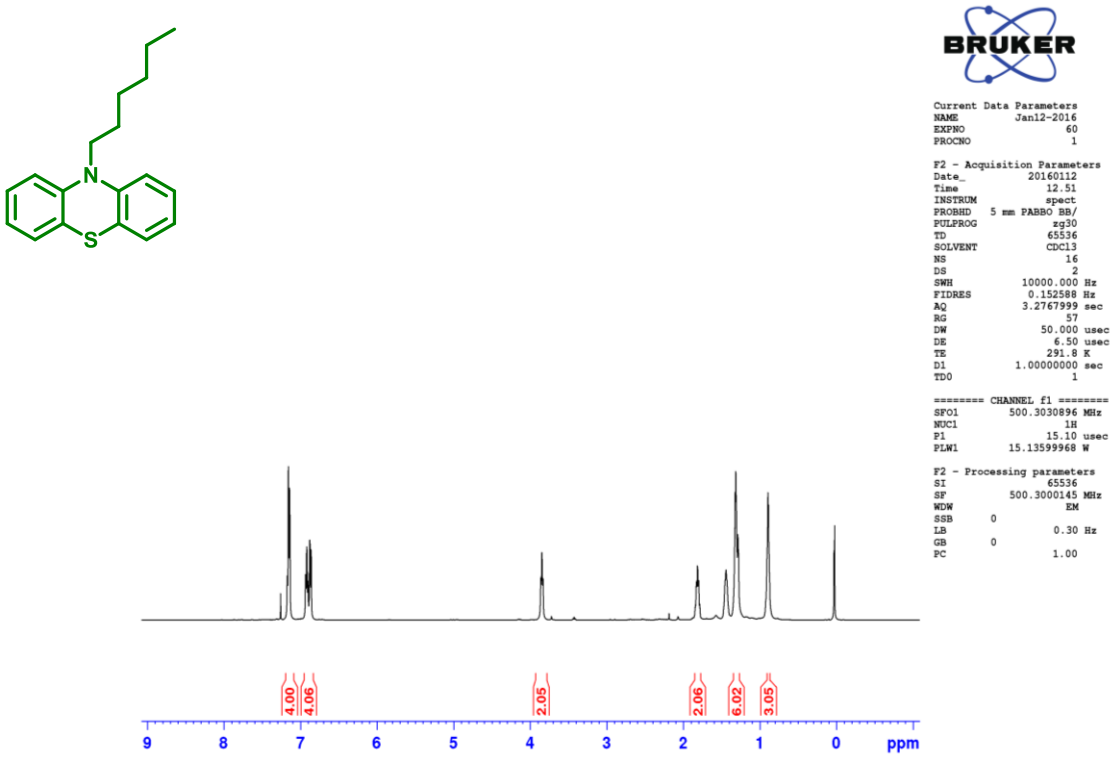

Fig.S6. ^{1}H NMR spectrum of 10-Hexyl-10H-phenothiazine, **Hexyl-PTZ** in $CDCl_3$.

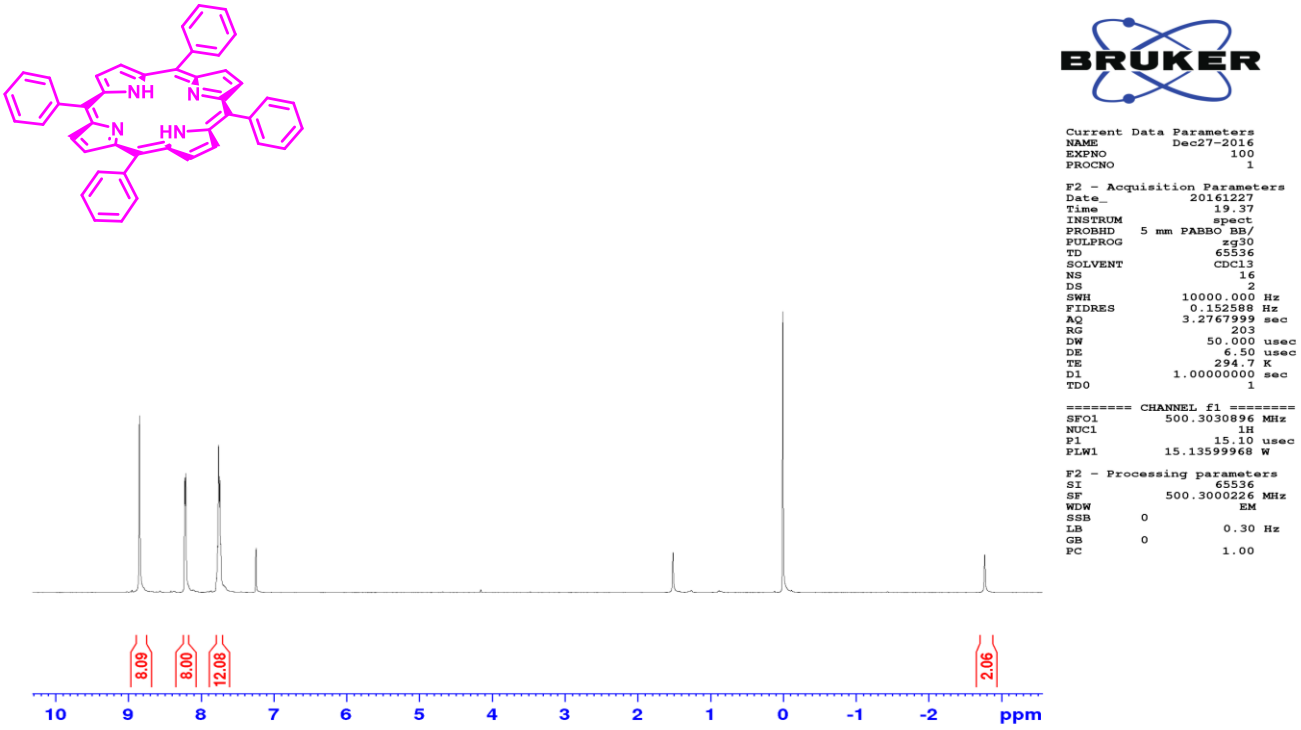

Fig.S7. ^{1}H NMR spectrum of 5, 10, 15, 20-tetra phenyl free base porphyrin, **H_2TPP** in $CDCl_3$.

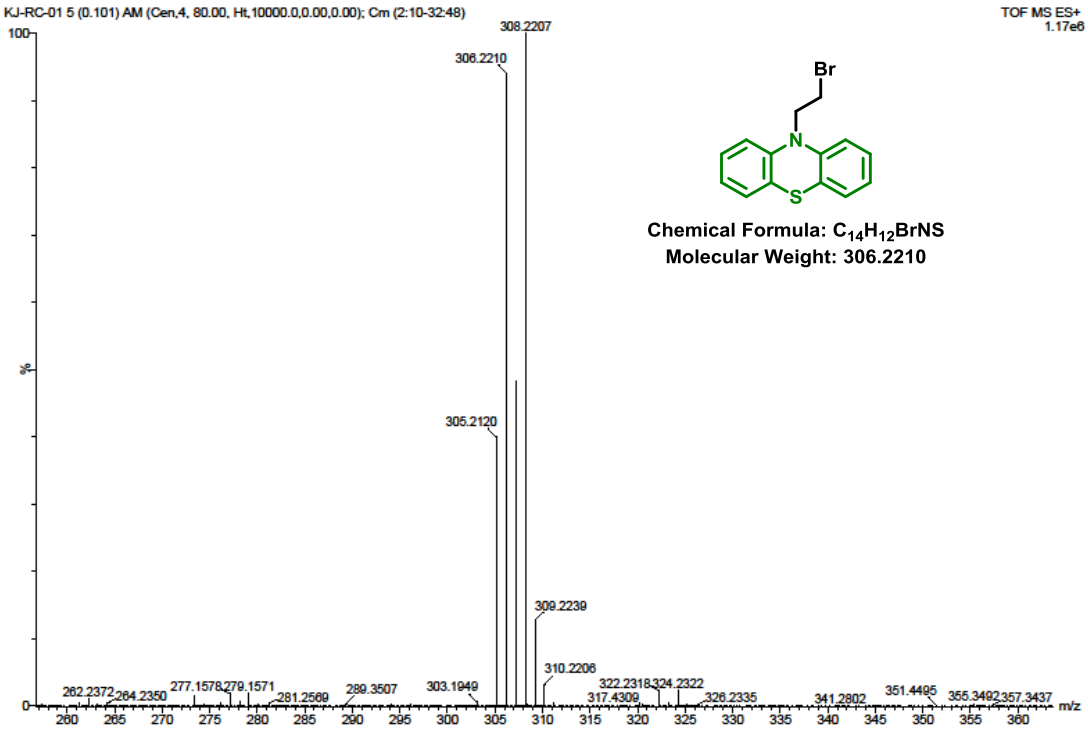

Fig.S8. HRMS (ESI) spectrum of 10-(2-bromoethyl)-10H-phenothiazine **(1)**.

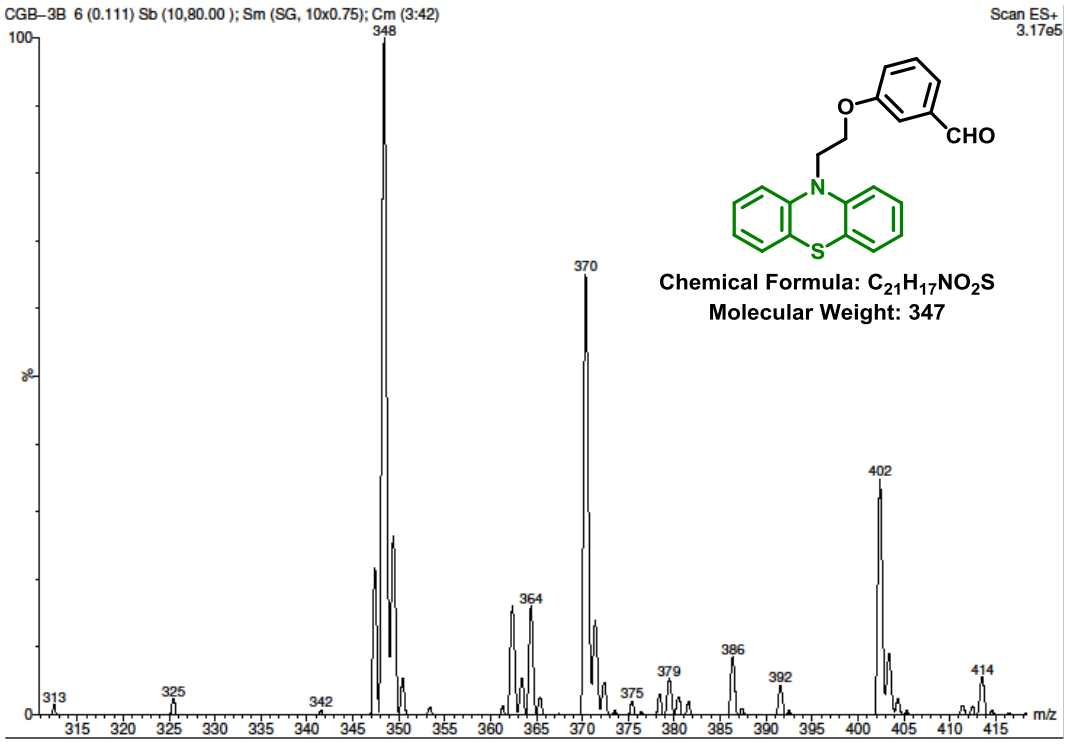

Fig. S9. ESI-MS spectrum of 3-(2-(10*H*-phenothiazin-10-yl)ethoxy)benzaldehyde**(2a)**.

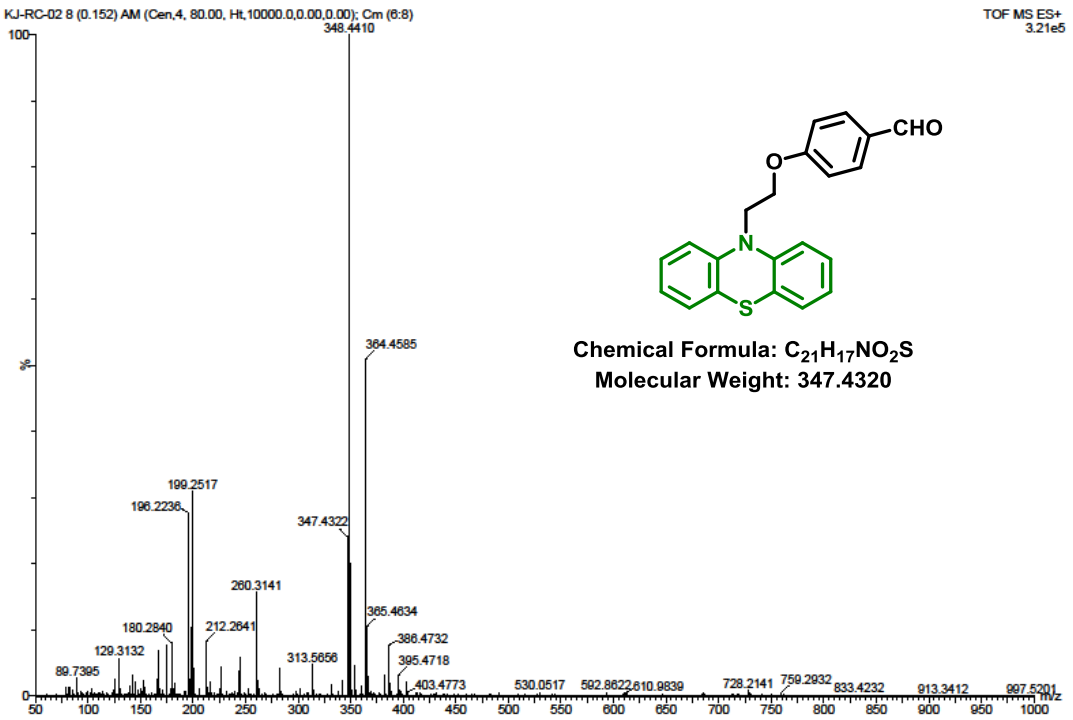

Fig.S10. HRMS (ESI) spectrum of 4-(2-(10*H*-phenothiazin-10-yl)ethoxy)benzaldehyde **(2b)**.

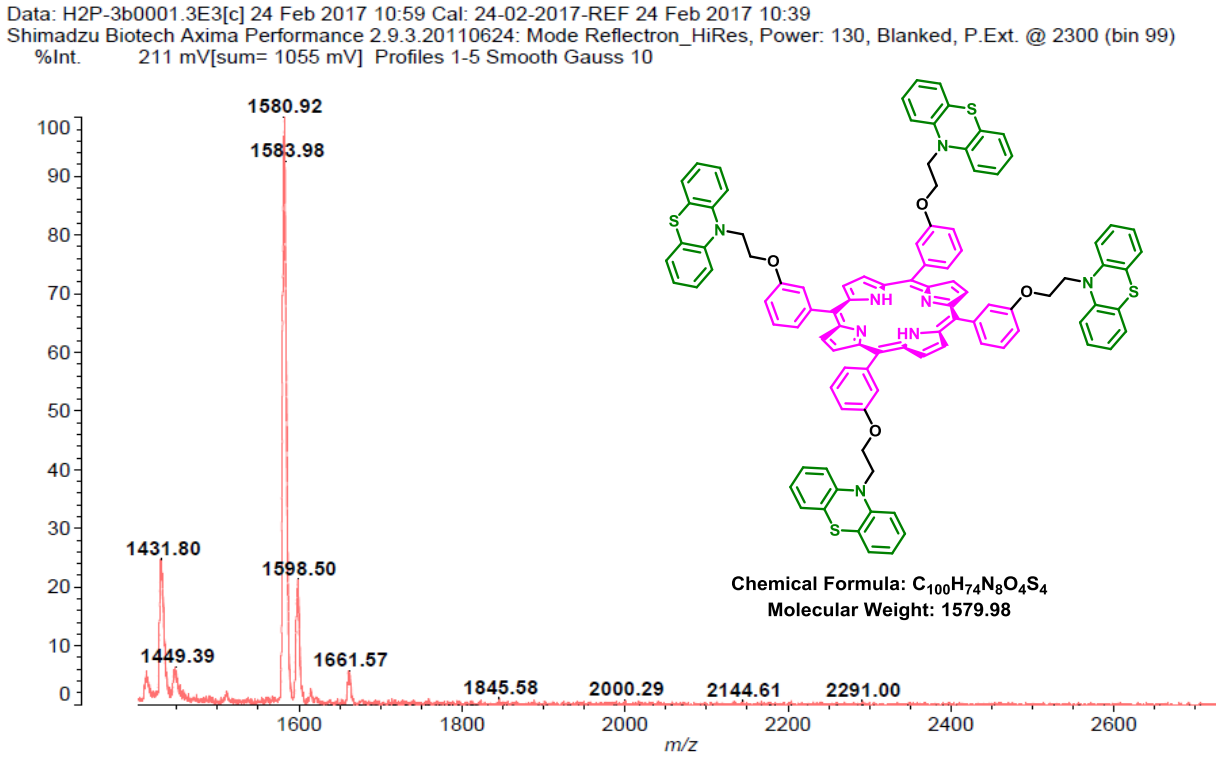

Fig. S11. MALDI-TOF spectrum of 5, 10, 15, 20-tetra-3-(2-(10H-phenothiazin-10-yl)ethoxy) phenyl free base porphyrin, ***m*-(PTZ)$_4$-H$_2$P**.

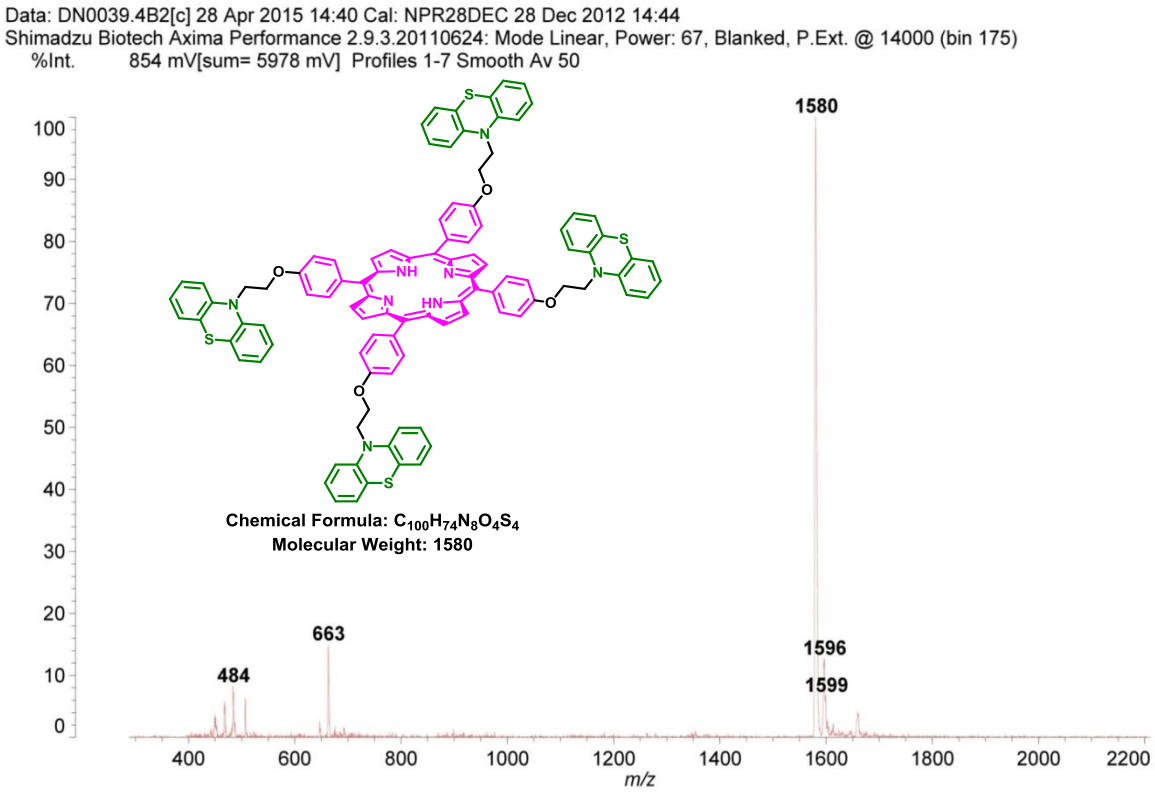

Fig. S12. MALDI-TOF spectrum of 5, 10, 15, 20-tetra-4-(2-(10H-phenothiazin-10-yl)ethoxy) phenyl free base porphyrin, ***p*-(PTZ)$_4$-H$_2$P**.

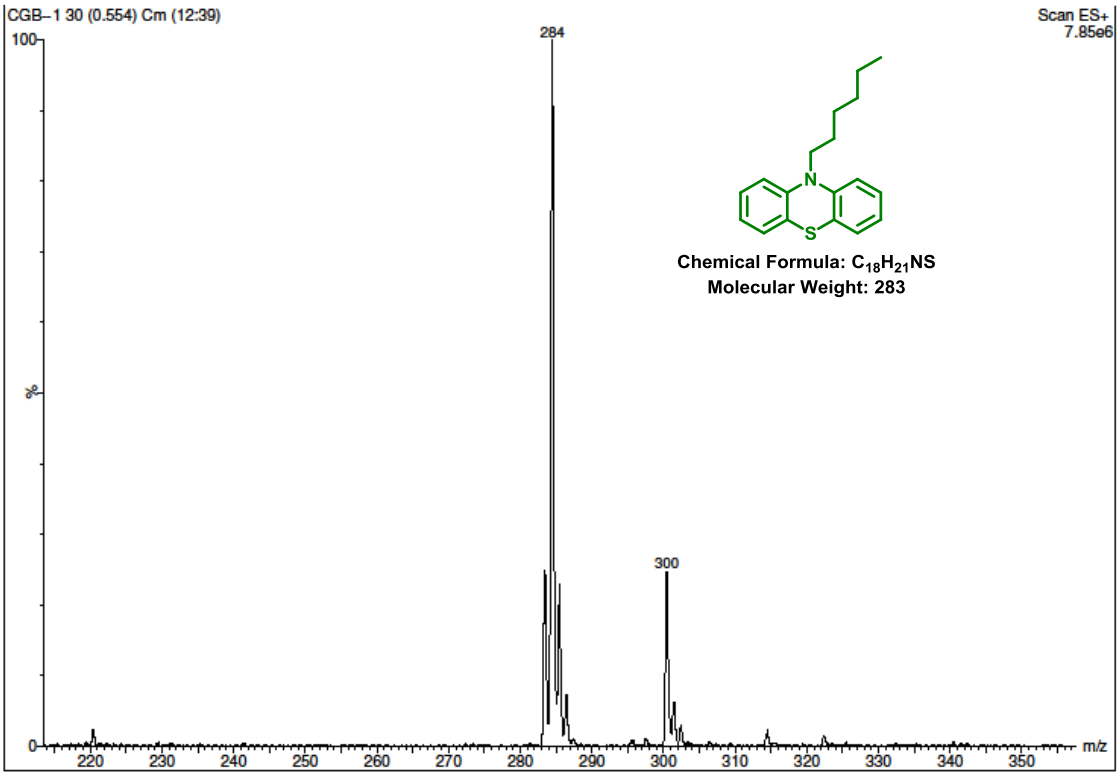

Fig. S13. ESI-MS spectrum of 10-(2-bromoethyl)-10H-phenothiazine, **(Hexyl-PTZ)**.

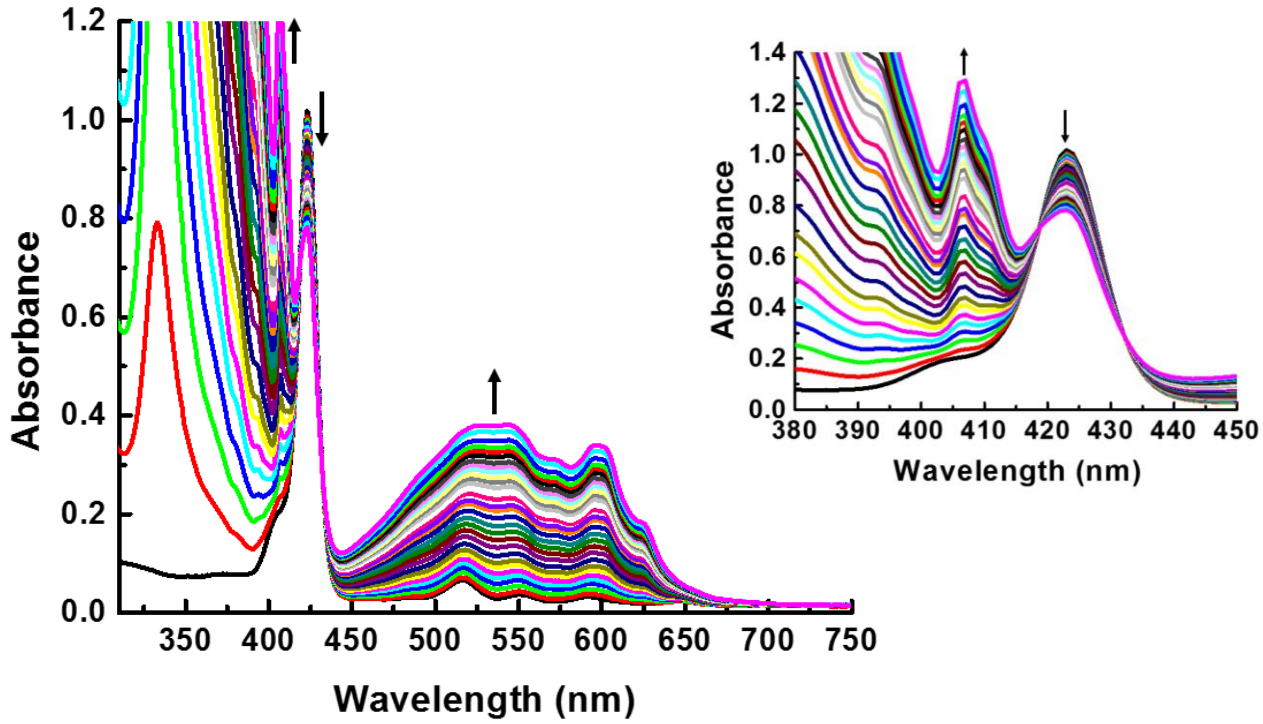

Fig. S14. Absorption titration of ***m*-(PTZ)$_4$-H$_2$P** (2.53×10^{-6} M) with increasing additions of **C$_{60}$** in 1,2-DCB.

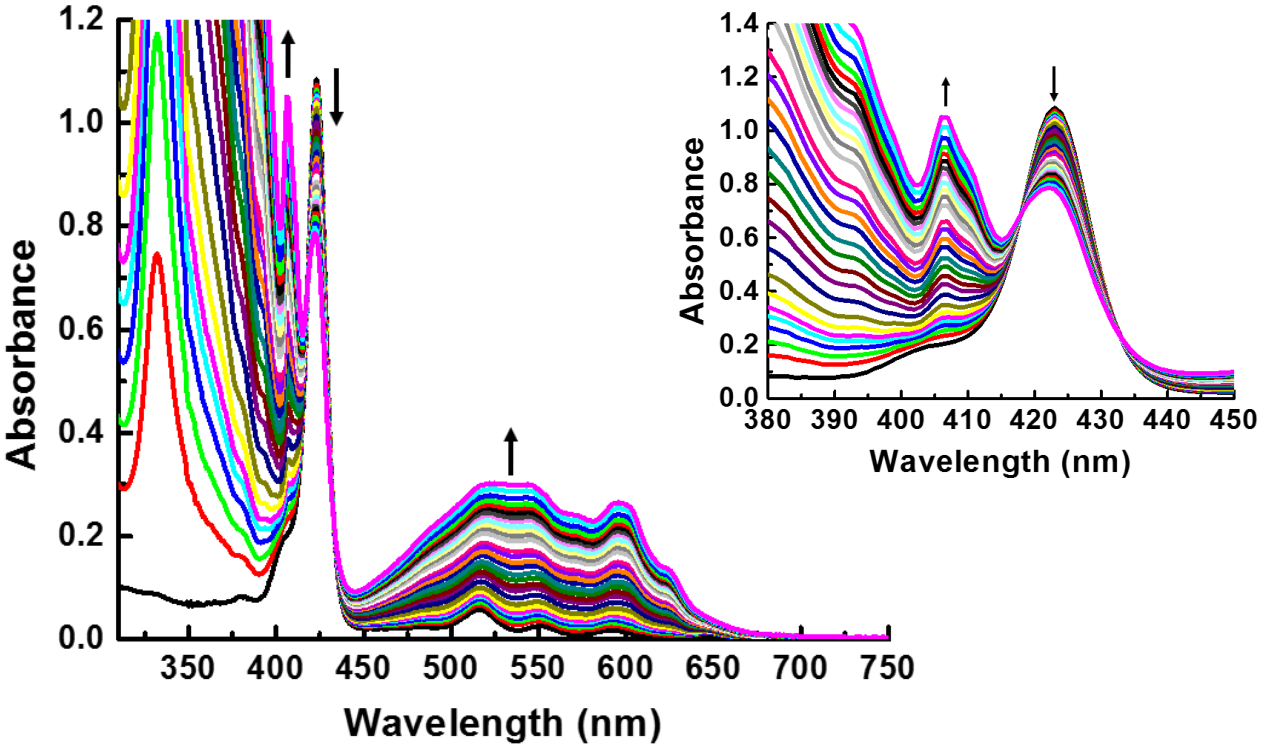

Fig. S15. Absorption titration of ***m*-(PTZ)$_4$-H$_2$P** (2.53×10^{-6} M) with increasing additions of **C$_{60}$** in PhCN.

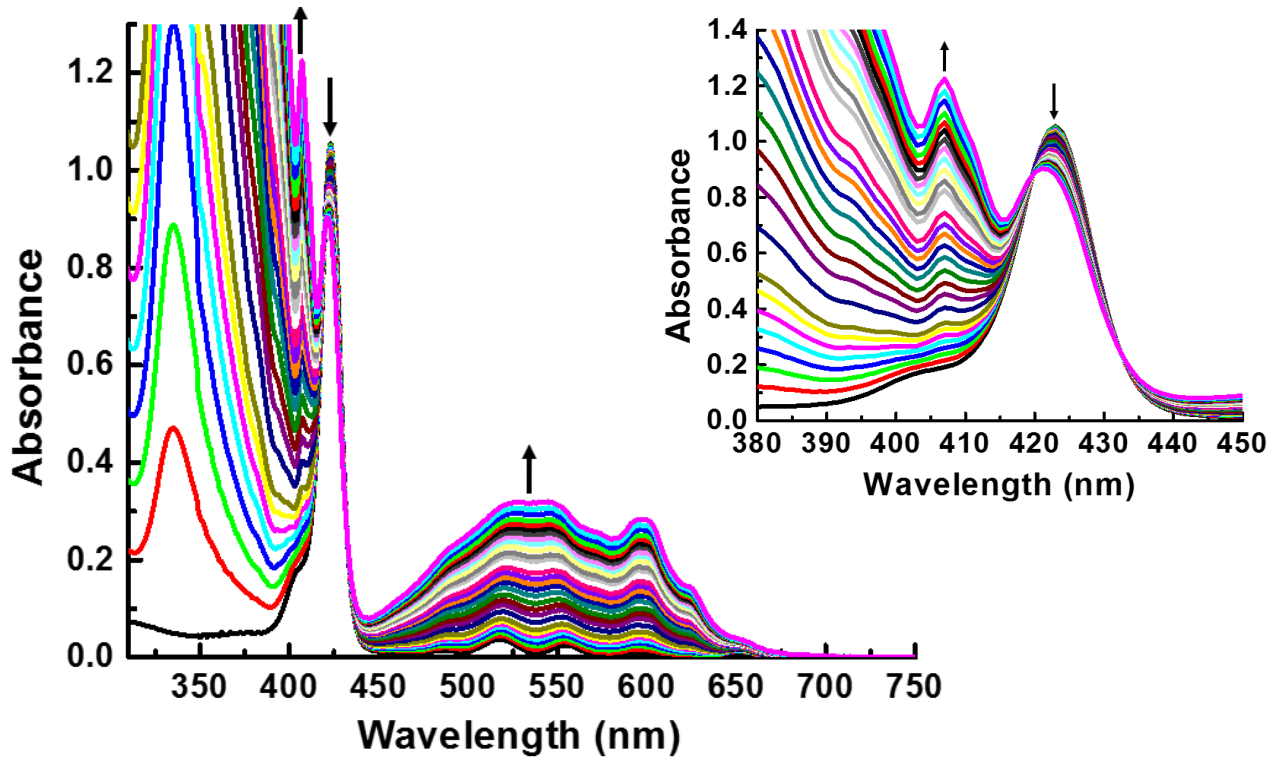

Fig. S16. Absorption titration of ***p*-(PTZ)$_4$-H$_2$P** (2.21×10^{-6} M) with increasing additions of **C$_{60}$** in toluene.

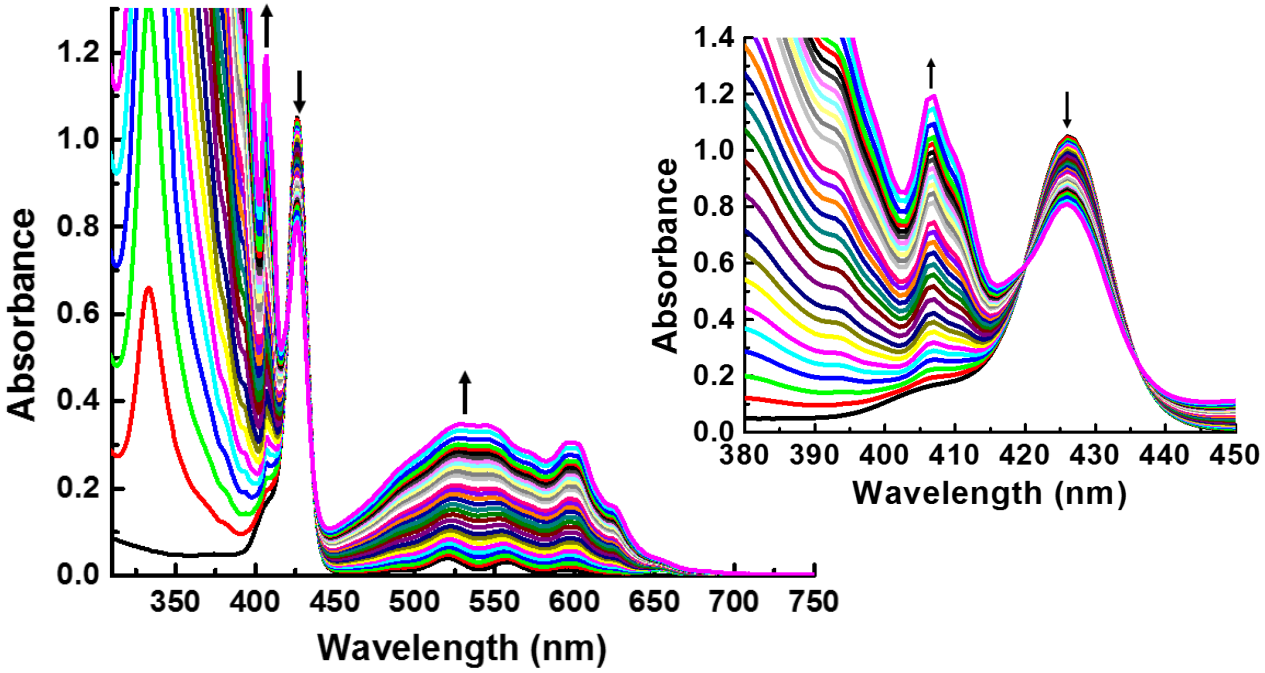

Fig. S17. Absorption titration of ***p*-(PTZ)$_4$-H$_2$P** (2.21×10^{-6} M) with increasing additions of **C$_{60}$** in 1,2-DCB.

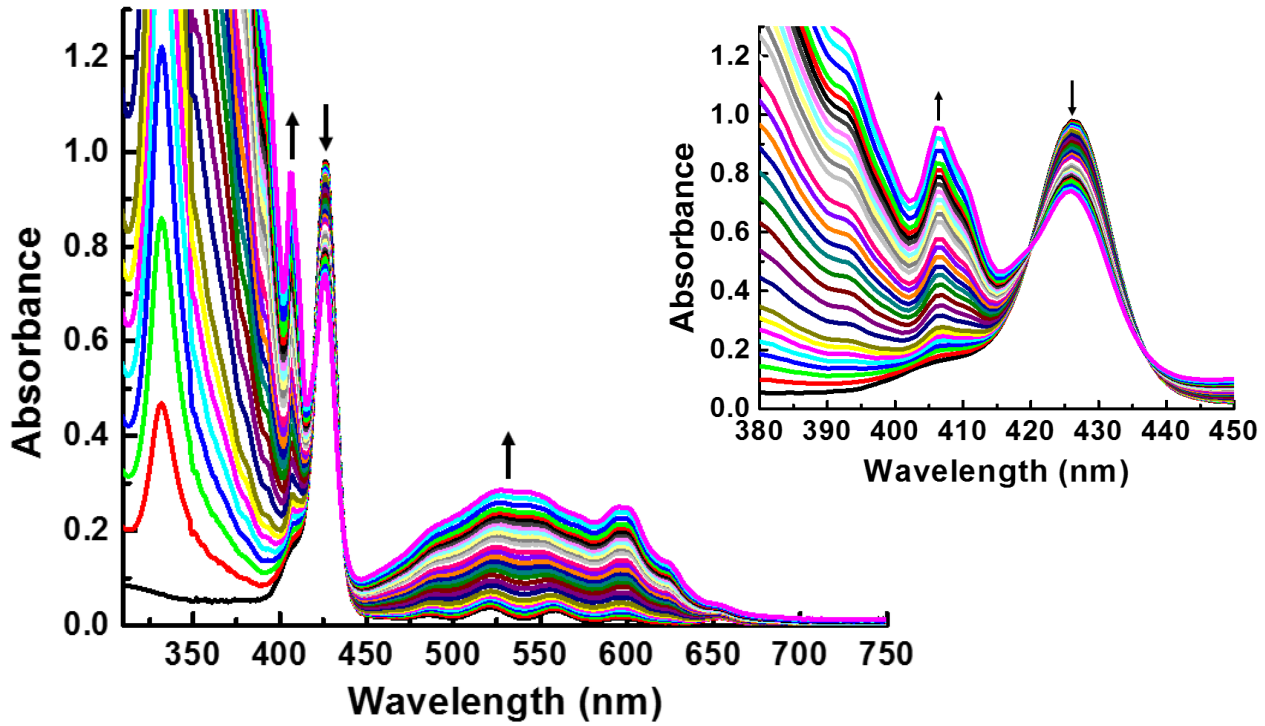

Fig. S18. Absorption titration of ***p*-(PTZ)$_4$-H$_2$P** (2.21×10^{-6} M) with increasing additions of **C$_{60}$** in PhCN.

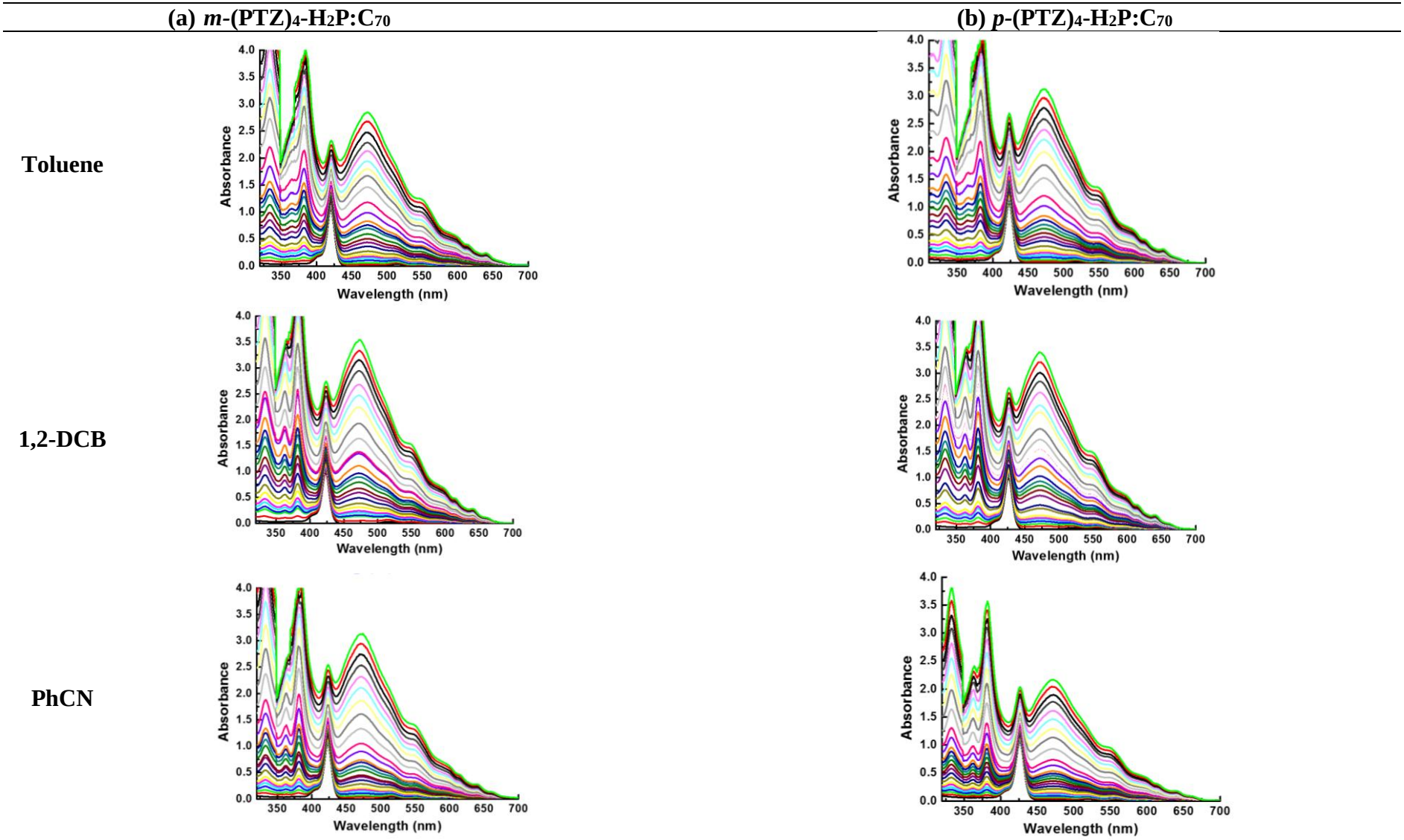

Fig. S19. Absorption titrations of (a) ***m*-(PTZ)$_4$-H$_2$P** (2.53×10^{-6} M) and (b) ***p*-(PTZ)$_4$-H$_2$P** (2.21×10^{-6} M) with increasing additions of **C$_{70}$** in toluene, 1,2-DCB, and PhCN.

Supporting Information

(a)

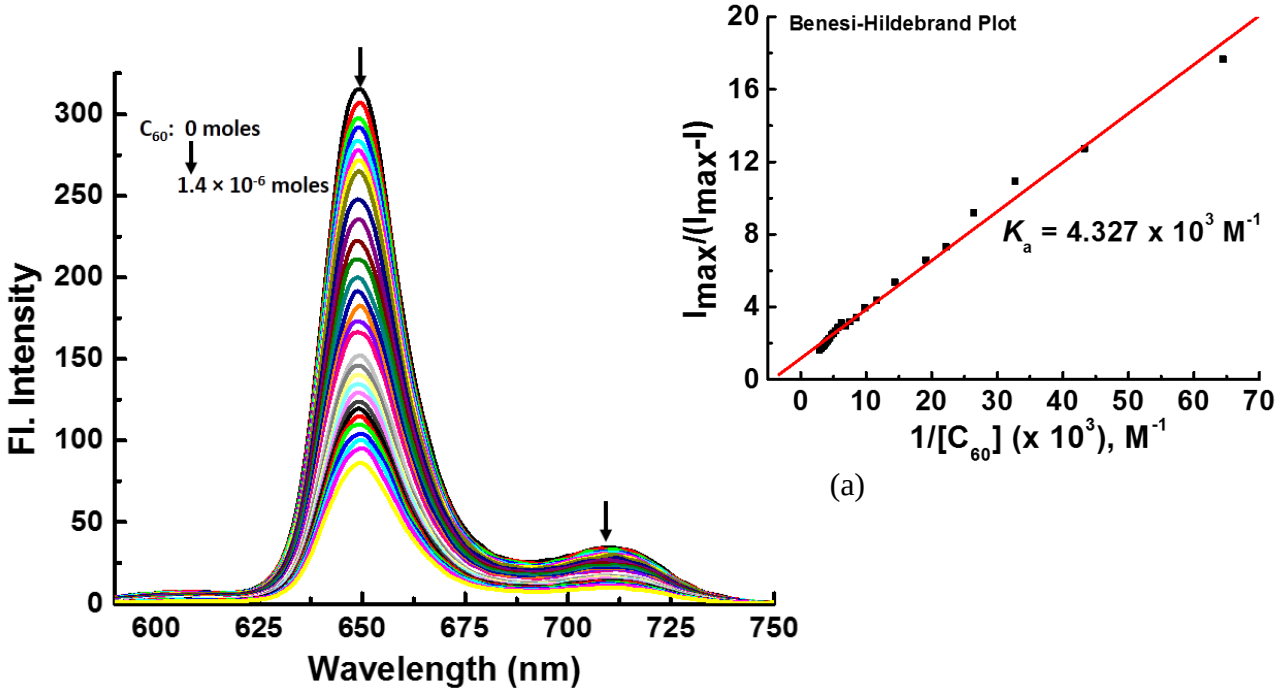

(b)

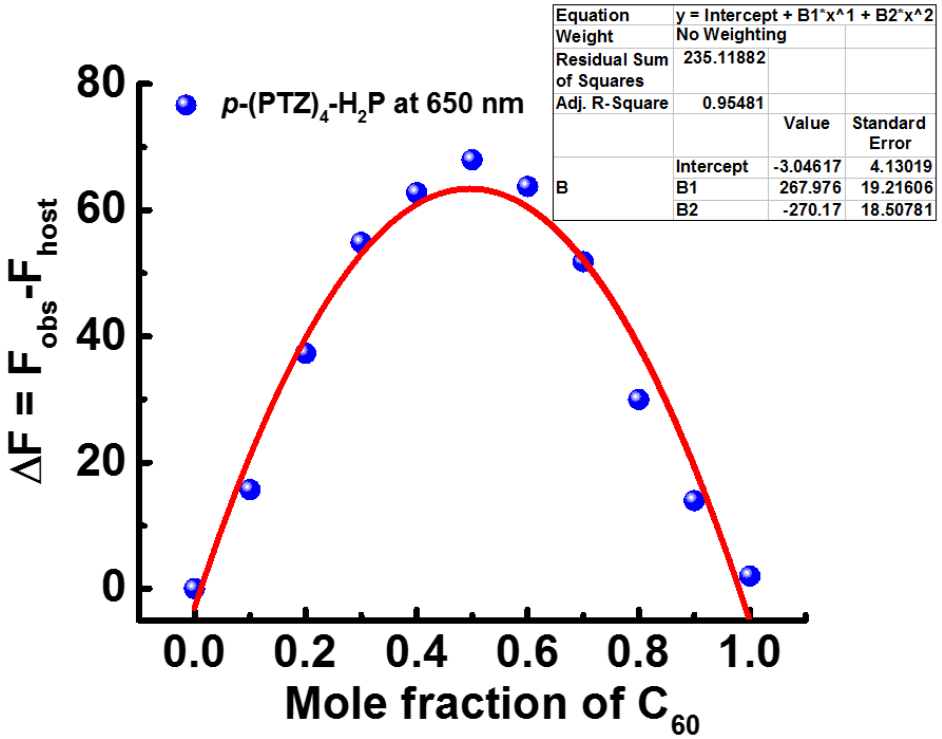

Fig. S20. (a) Fluorescence titration of ***m*-(PTZ)$_4$-H$_2$P** (2.53×10^{-6} M, λ_{ex}: 515 nm) with increasing additions of **C$_{60}$** in toluene. The inset shows the Benesi-Hildebrand plot of the change of fluorescence intensity at 650 nm, and (b) Job plot of continuous variation for ***m*-(PTZ)$_4$-H$_2$P:C$_{60}$** in toluene. Y-axis is the difference between the fluorescence intensities of the complex and ***m*-(PTZ)$_4$-H$_2$P** at 650 nm.

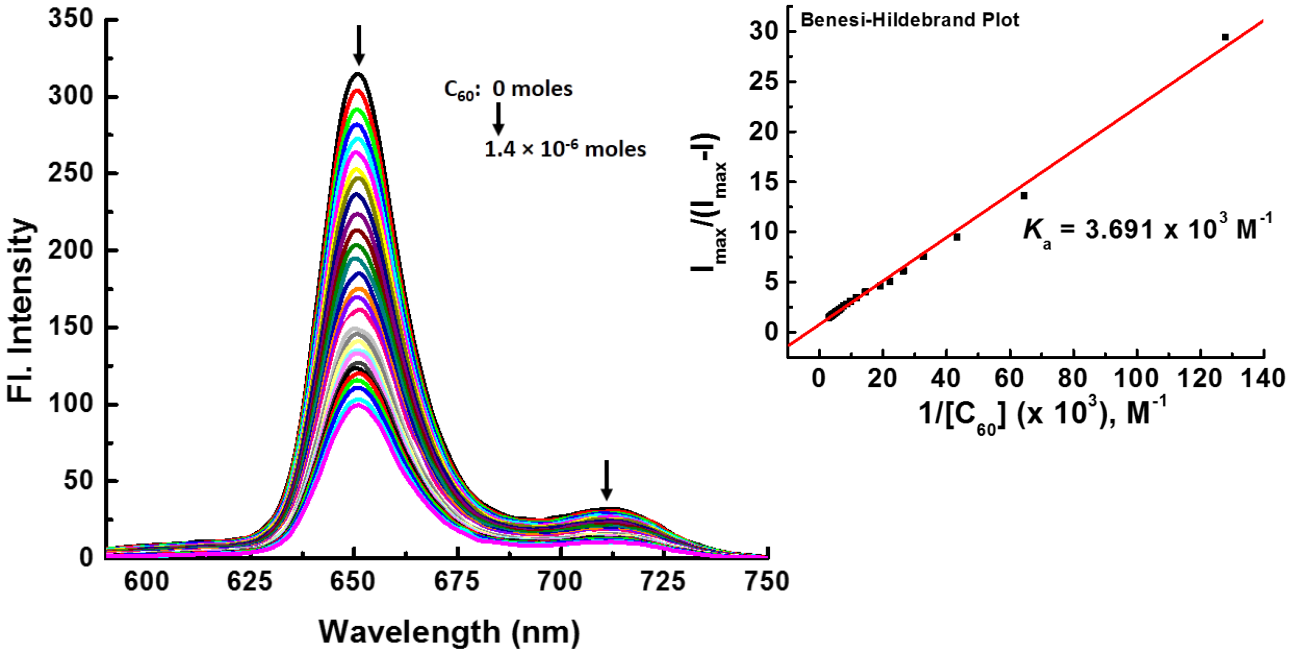

Fig. S21. Fluorescence titration of ***m*-(PTZ)$_4$-H$_2$P** (2.53×10^{-6} M, λ_{ex}: 515 nm) with increasing additions of **C$_{60}$** in 1,2-DCB. The inset shows the Benesi-Hildebrand plot of the changes of fluorescence intensity at 650 nm.

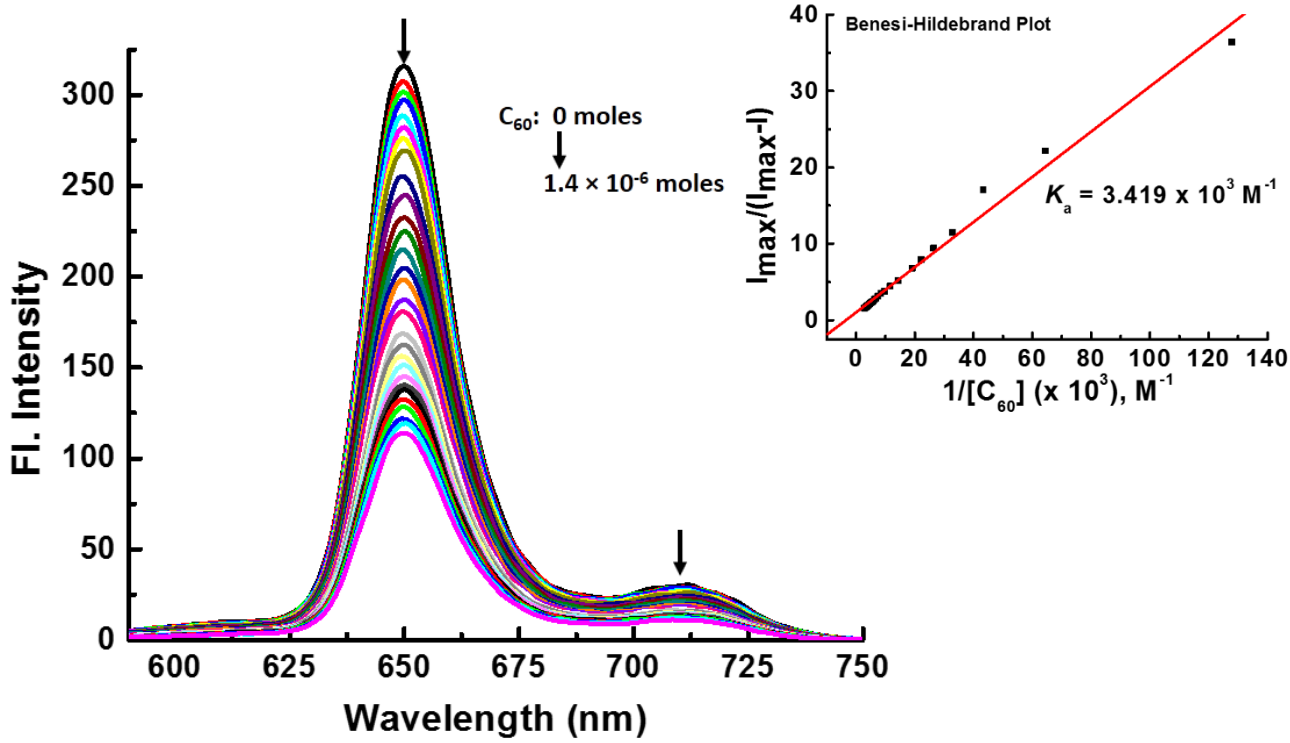

Fig. S22. Fluorescence titration of ***m*-(PTZ)$_4$-H$_2$P** (2.53×10^{-6} M, λ_{ex}: 515 nm) with increasing additions of **C$_{60}$** in PhCN. The inset shows the Benesi-Hildebrand plot of the change of fluorescence intensity at 650 nm.

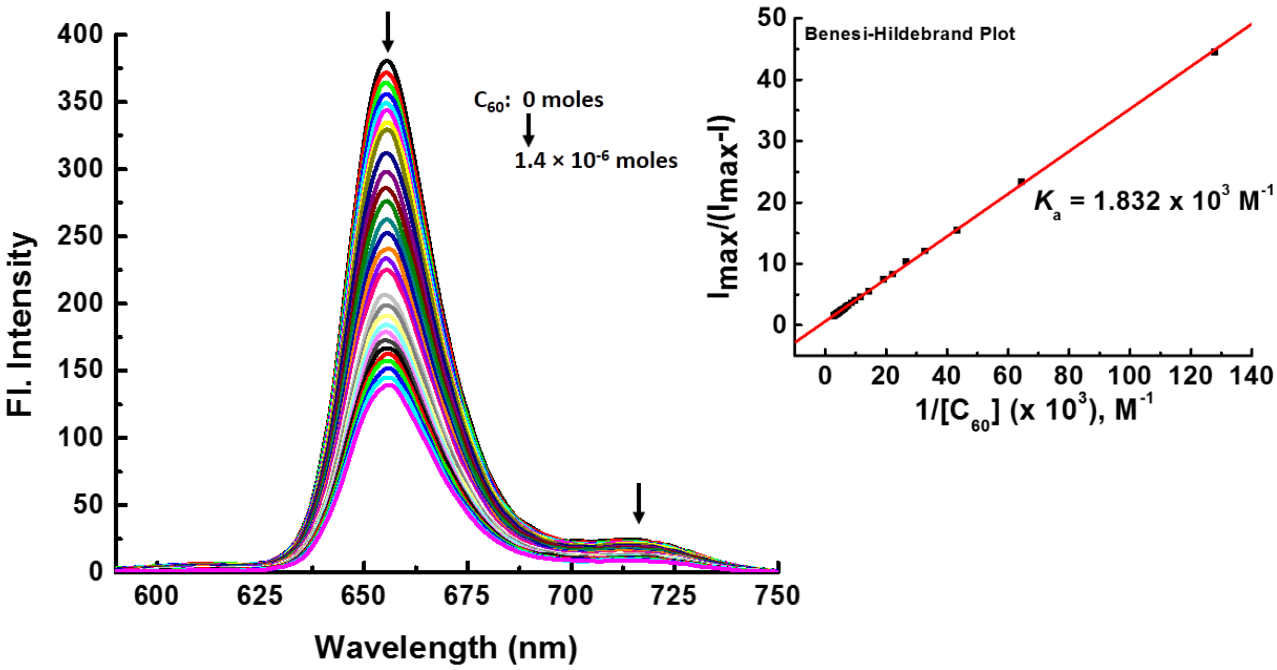

Fig. S23. Fluorescence titration of ***p*-(PTZ)$_4$-H$_2$P** (2.21×10^{-6} M, λ_{ex}: 515 nm) with increasing additions of **C$_{60}$** in toluene. The inset shows the Benesi-Hildebrand plot of the change of fluorescence intensity at 656 nm.

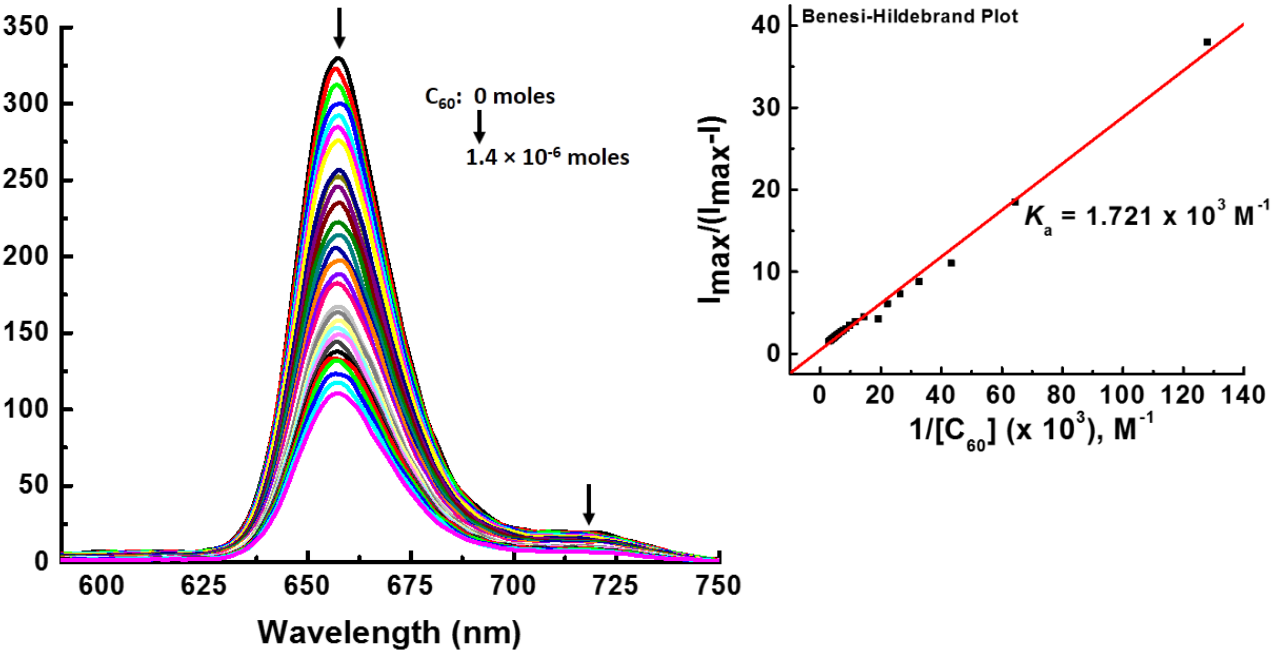

Fig. S24. Fluorescence titration of ***p*-(PTZ)$_4$-H$_2$P** (2.21×10^{-6} M, λ_{ex}: 515 nm) with increasing additions of **C$_{60}$** in 1,2-DCB. The inset shows the Benesi-Hildebrand plot of the change of fluorescence intensity at 658 nm.

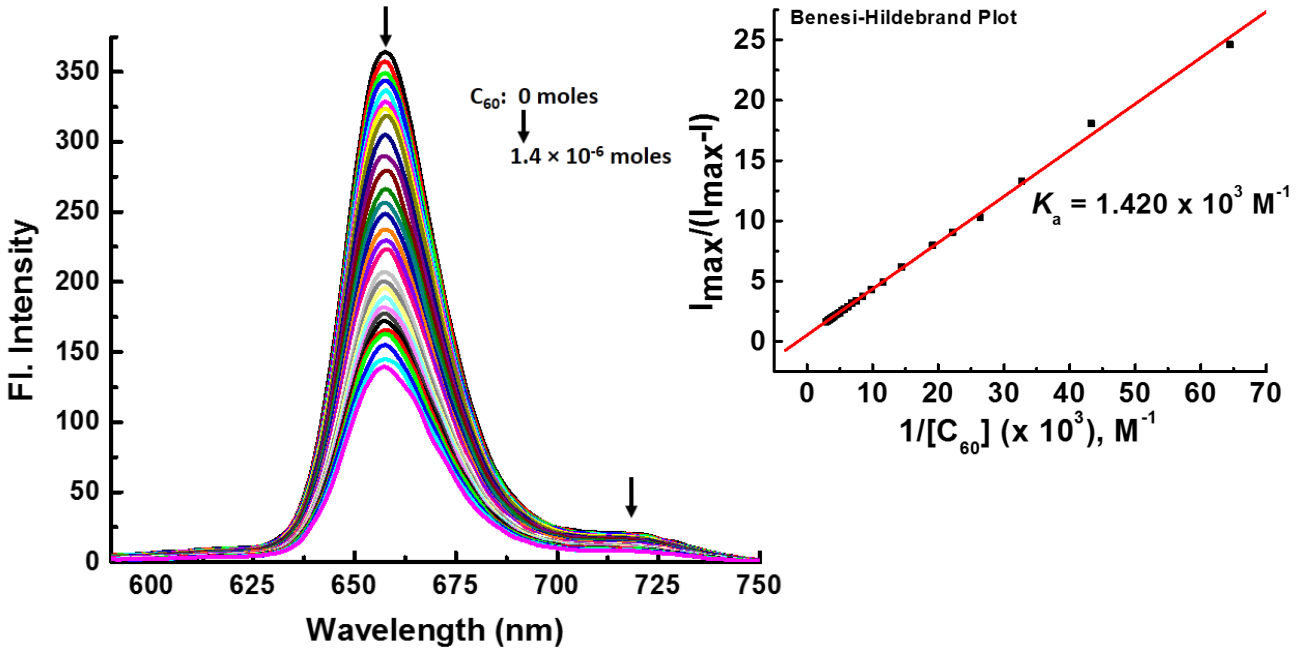

Fig. S25. Fluorescence titration of ***p*-(PTZ)$_4$-H$_2$P** (2.21×10^{-6} M, λ_{ex}: 515 nm) with increasing additions of **C$_{60}$** in PhCN. The inset shows the Benesi-Hildebrand plot of the change of fluorescence intensity at 658 nm.

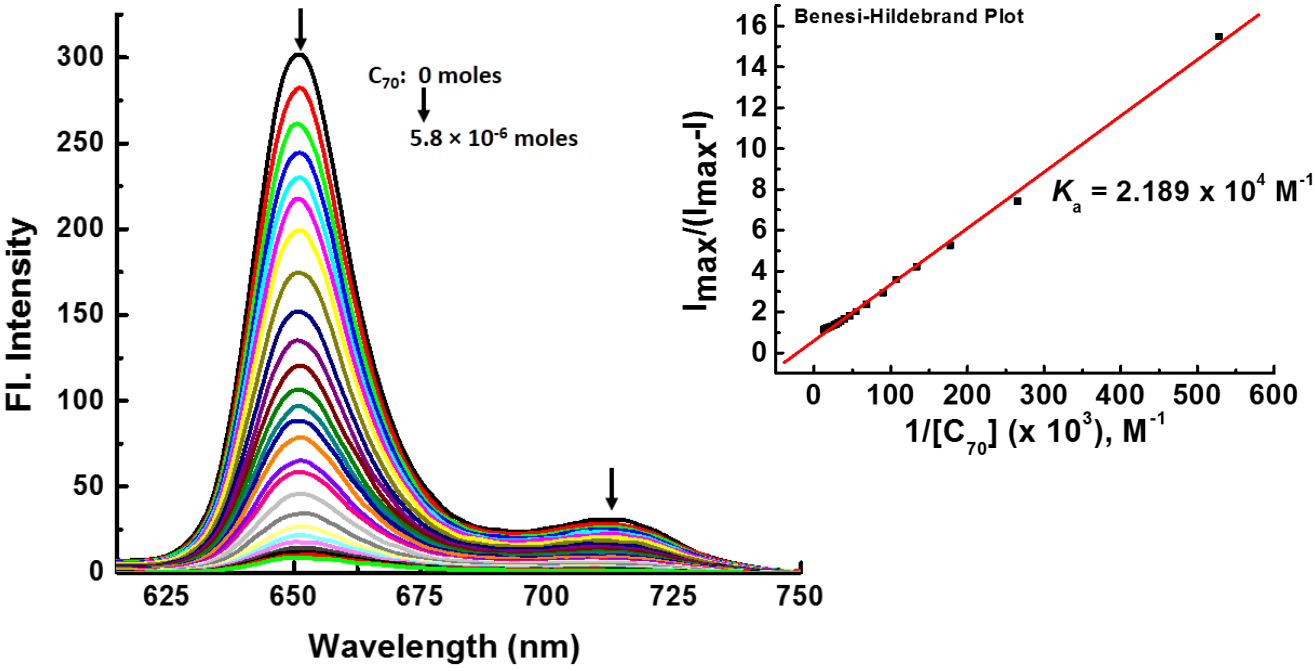

Fig. S26. Fluorescence titration of ***m*-(PTZ)$_4$-H$_2$P** (2.53×10^{-6} M, λ_{ex}: 515 nm) with increasing additions of **C$_{70}$** in 1,2-DCB. The inset shows the Benesi-Hildebrand plot of the change of fluorescence intensity at 651 nm.

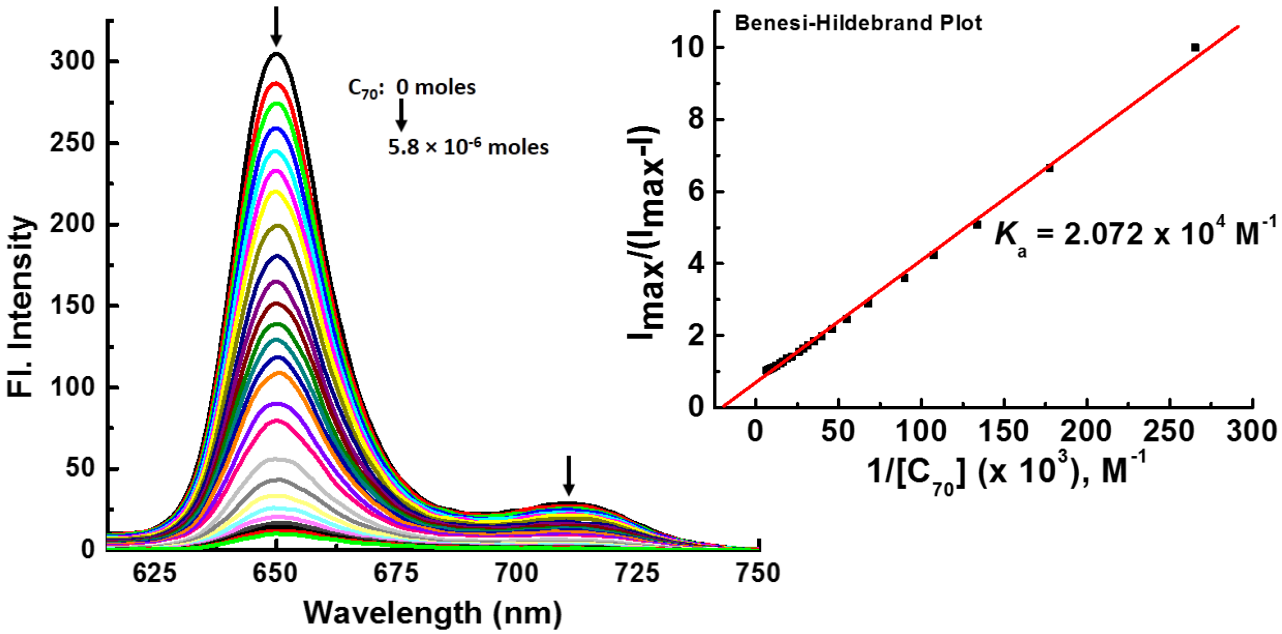

Fig. S27. Fluorescence titration of ***m*-(PTZ)$_4$-H$_2$P** (2.53 × 10^{-6} M, λ_{ex}: 515 nm) with increasing additions of **C$_{70}$** in PhCN. The inset shows the Benesi-Hildebrand plot of the change of fluorescence intensity at 650 nm.

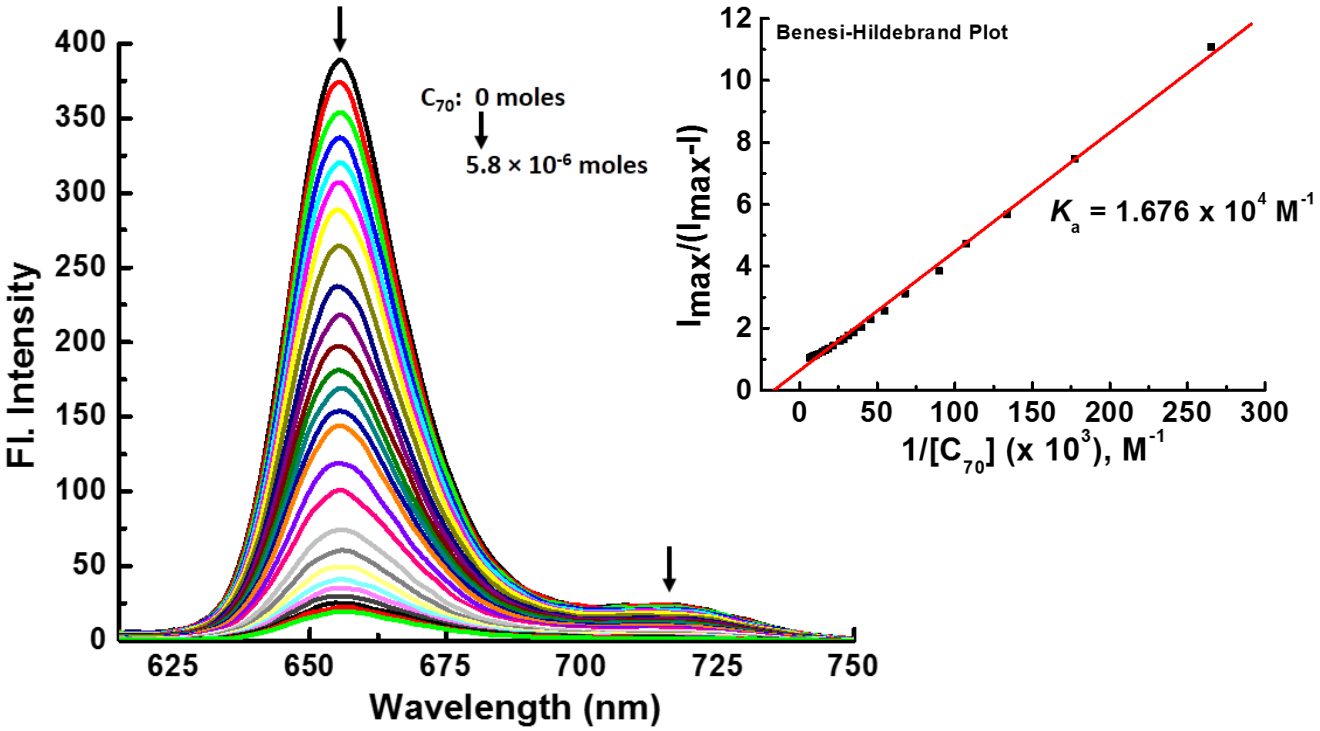

Fig. S28. Fluorescence titration of ***p*-(PTZ)$_4$-H$_2$P** (2.21 × 10^{-6} M, λ_{ex}: 515 nm) with increasing additions of **C$_{70}$** in toluene. The inset shows the Benesi-Hildebrand plot of the change of fluorescence intensity at 656 nm.

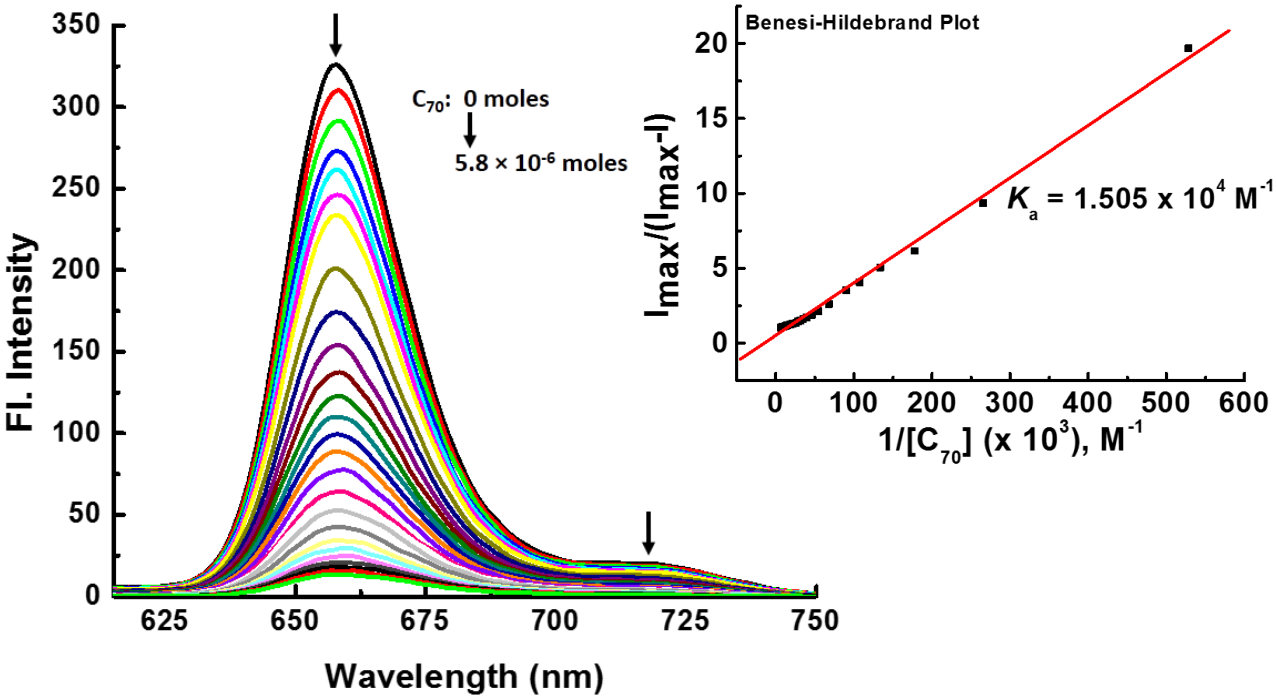

Fig. S29. Fluorescence titration of ***p*-(PTZ)$_4$-H$_2$P** (2.21 × 10^{-6} M, λ_{ex}: 515 nm) with increasing additions of **C$_{70}$** in 1,2-DCB. The inset shows the Benesi-Hildebrand plot of the change of fluorescence intensity at 658 nm.

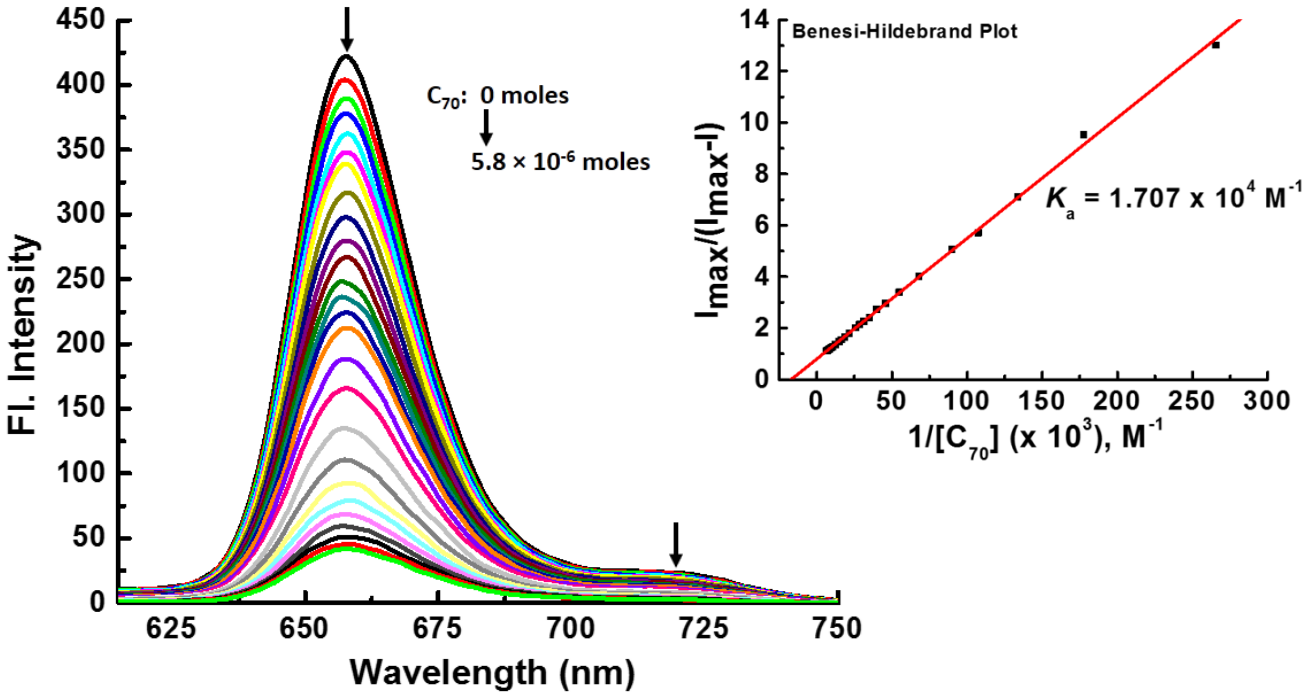

Fig. S30. Fluorescence titration of ***p*-(PTZ)$_4$-H$_2$P** (2.21 × 10^{-6} M, λ_{ex}: 515 nm) with increasing additions of **C$_{70}$** in PhCN. The inset shows the Benesi-Hildebrand plot of the change of fluorescence intensity at 658 nm.

Supporting Information

Table S1: Binding constants (reported) of the porphyrin receptors with C_{60} and C_{70} in different solvents.

Host	**Solvent**	**Binding Constant (M^{-1})**	
		C_{60}	C_{70}
(18-crown-6)$_4$-H_2P[1]	PhCN	5.6×10^3 [a]	--
	1,2-DCB	6.9×10^3 [a]	--
	toluene	7.9×10^3 [a]	--
(coronene)$_4$-H_2P[2]	toluene-d_8	$(5.4 \pm 0.2) \times 10^3$ [b]	
(pyrene)$_8$-ZnP[3] (1:1 model)	toluene-d_8	$K_1 = (2.30 \pm 0.01) \times 10^3$ [c]	$K_1 = (2.69 \pm 0.02) \times 10^4$ [c]
(pyrene)$_8$-H_2P[3] (1:2 model)		$K_1 = (1.49 \pm 0.01) \times 10^3$ [c]	$K_1 = (1.40 \pm 0.05) \times 10^4$ [c]
		$K_2 = (3.71 \pm 0.02) \times 10^2$ [c]	$K_2 = (3.50 \pm 0.13) \times 10^3$ [c]

[1] F. D'Souza, R. Chitta, S. Gadde, M. E. Zandler, A. L. McCarty, A. S. Sandanayaka, Y. Araki, O. Ito, *J. Phys. Chem. A.,* 2006, **110**, 4338-4347; [a]: calculated from fluorescence titration.

[2] C. M. Alvarez, H. Barbero, S. Ferrero, D. Miguel, *J. Org. Chem.*, 2016, **81**, 6081-6086; [b]: calculated from ^{1}H NMR titration.

[3] S. Ferrero, H. Barbero, D. Miguel, R. Garcia-Rodriguez, C. M. Alvarez, *J. Org. Chem.*, 2019, **84**, 6183-6190; [c]: calculated from ^{1}H NMR titration.

(a) 1,2-DCB

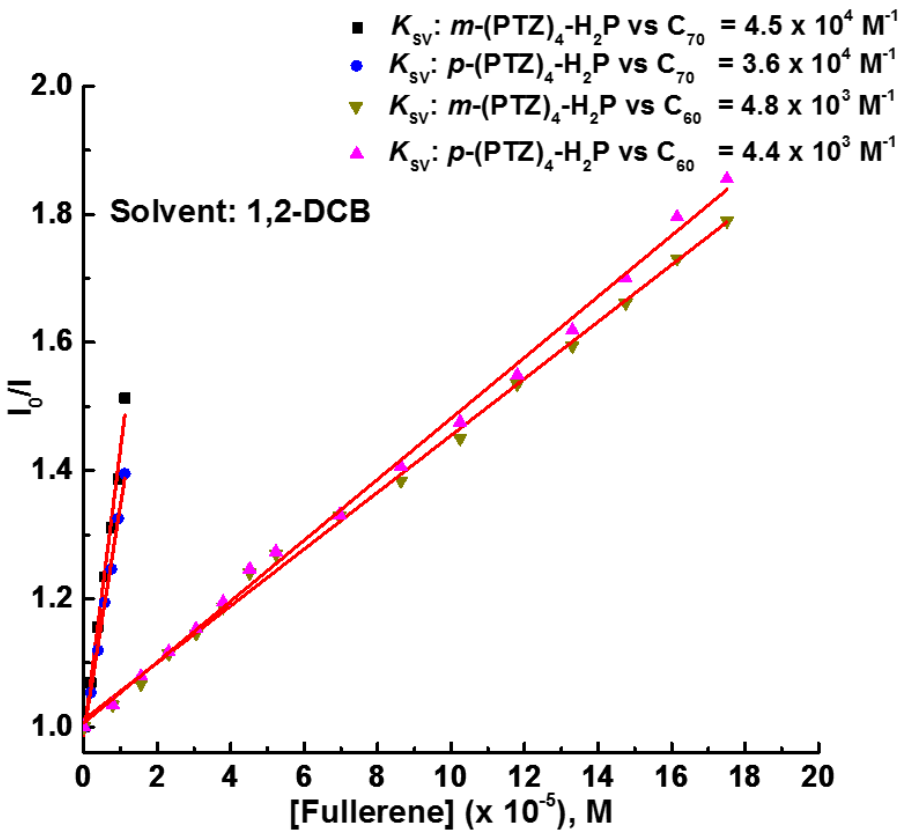

(b) PhCN

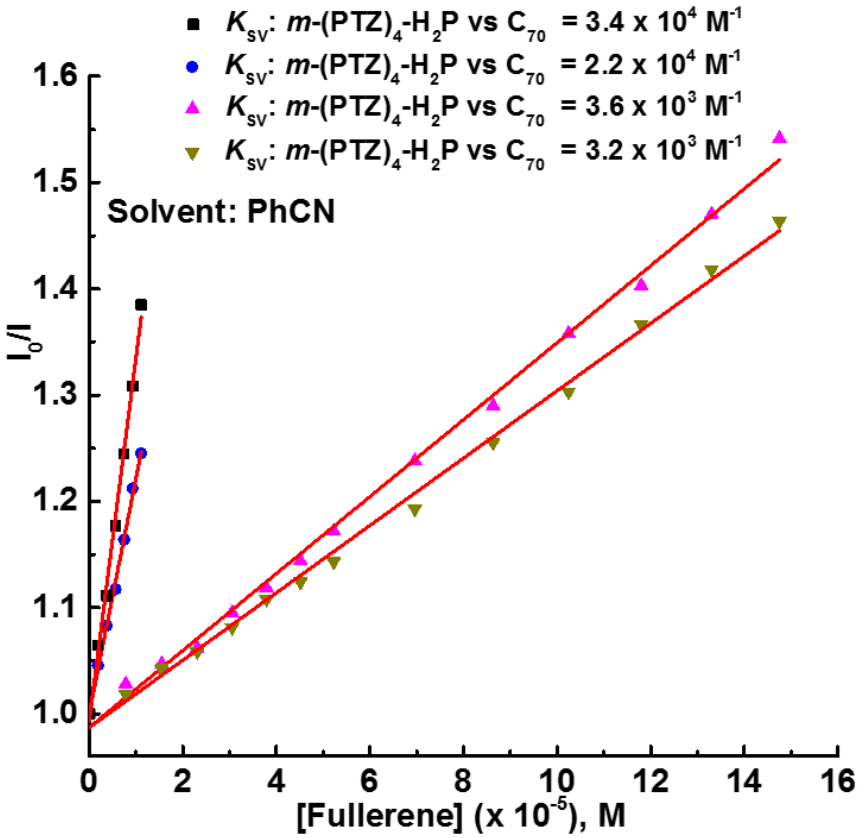

Fig. S31. Stern-Volmer quenching plots of fluorescence quenching at 650 nm of ***m*-(PTZ)$_4$-H$_2$P** and ***p*-(PTZ)$_4$-H$_2$P** by **C$_{70}$** and **C$_{60}$** in (a) 1,2-DCB and (b) PhCN. λ_{ex}: 515 nm.

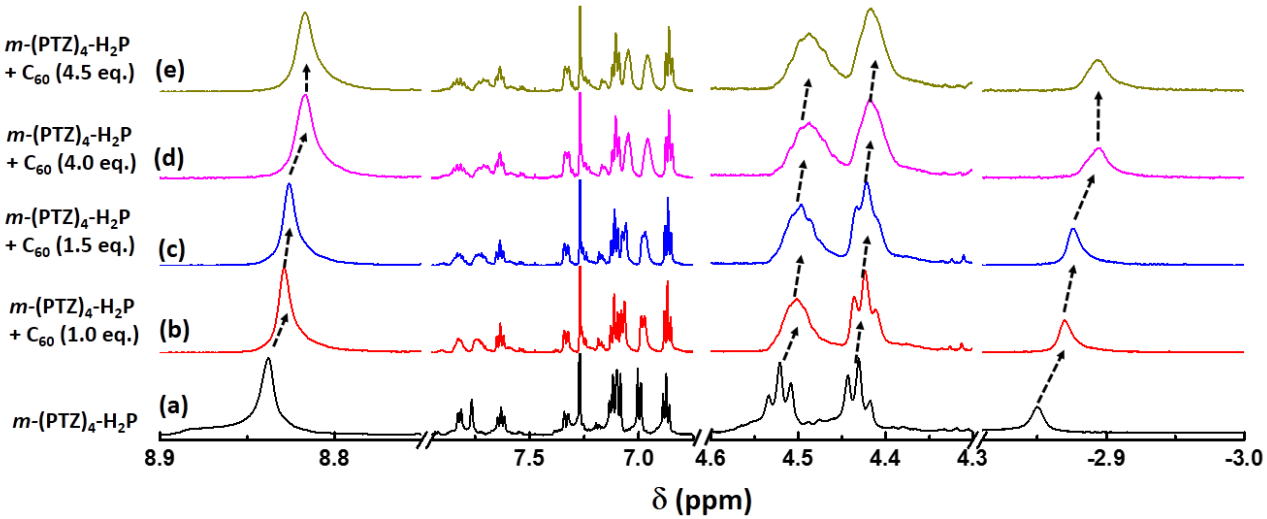

Fig. S32. ^{1}H NMR spectrum of (a) ***m*-(PTZ)$_4$-H$_2$P** (0.62×10^{-6} moles) in $CDCl_3$, and (b)-(e) upon addition of 1.0, 1.5, 4.0, 4.5 eq. of **C$_{60}$** in $CDCl_3$.

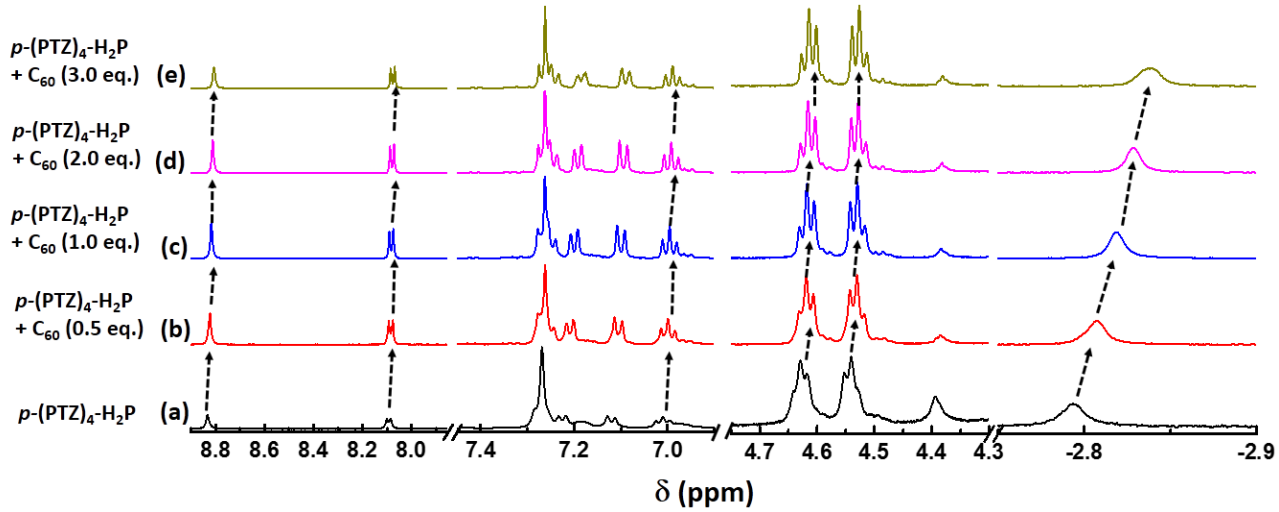

Fig. S33. ^{1}H NMR spectrum of (a) ***p*-(PTZ)$_4$-H$_2$P** (1.2×10^{-6} moles) in $CDCl_3$, and (b)-(e) upon addition of 0.5, 1.0, 2.0, 3.0 eq. of **C$_{60}$** in $CDCl_3$.

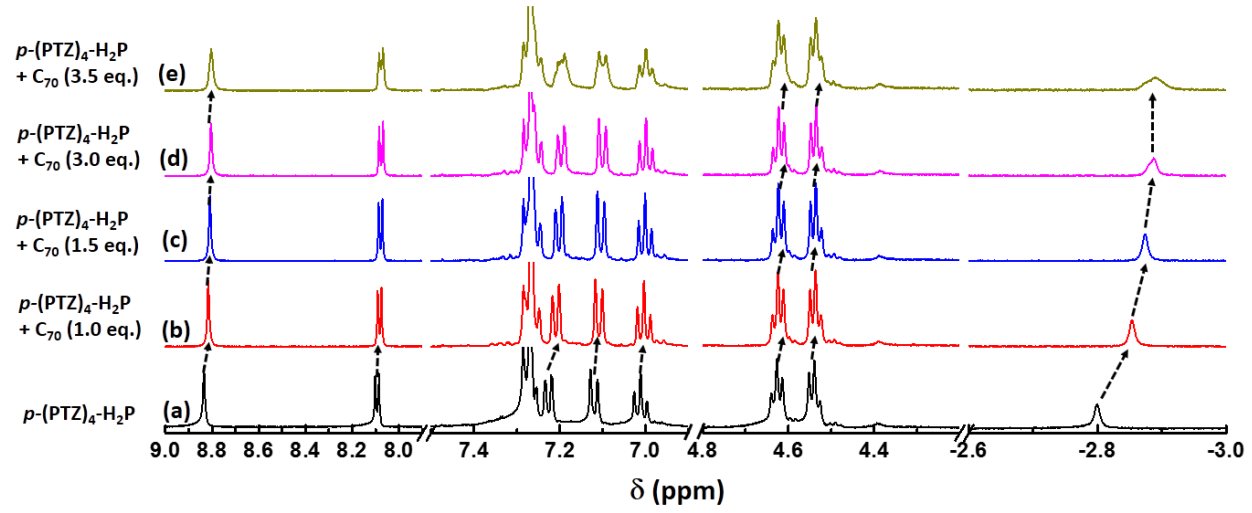

Fig. S34. ^{1}H NMR spectrum of (a) ***p*-(PTZ)$_4$-H$_2$P** (1.2×10^{-6} moles) in $CDCl_3$, and (b)-(e) upon addition of 1.0, 1.5, 3.0, 3.5 eq. of **C$_{70}$** in $CDCl_3$.

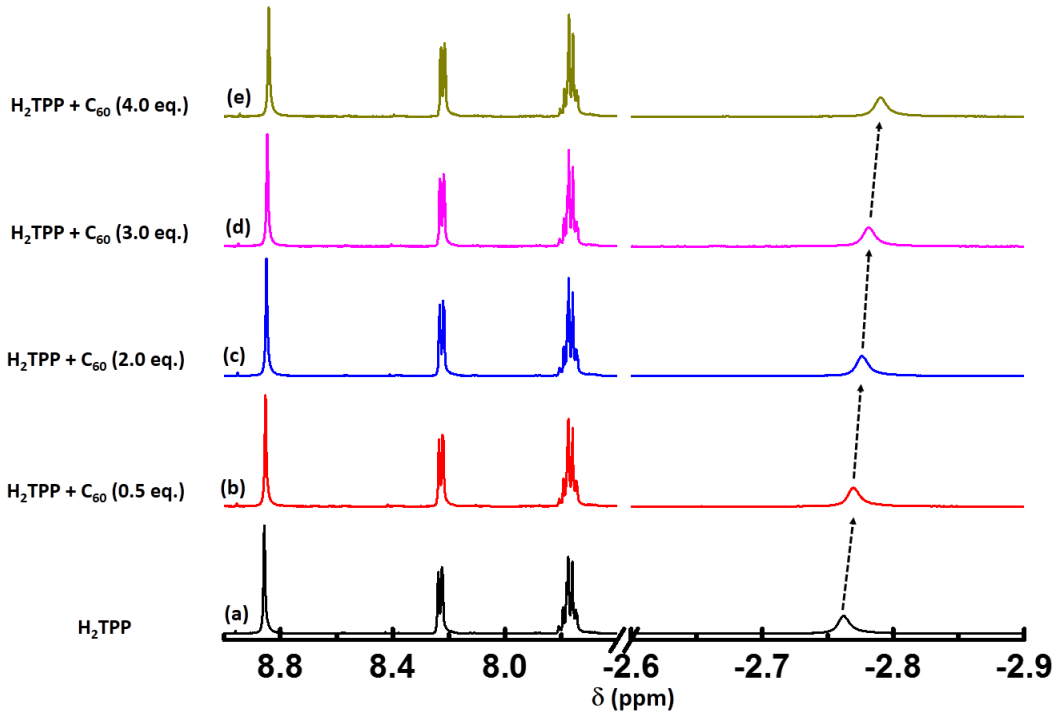

Fig. S35. ^{1}H NMR spectrum of (a) **H_2TPP** (0.62×10^{-6} moles) in $CDCl_3$, and (b)-(e) upon addition of 0.5, 2.0, 3.0, 4.0 eq. of **C_{60}** in $CDCl_3$.

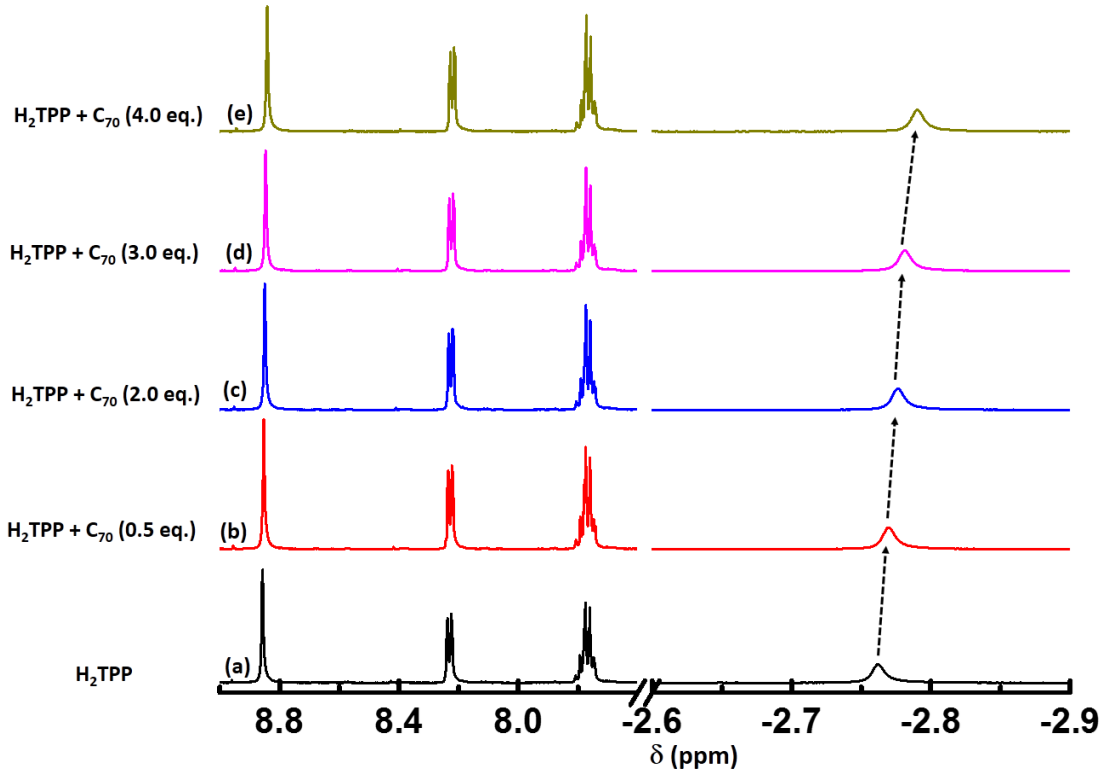

Fig. S36. ^{1}H NMR spectrum of (a) **H_2TPP** (0.62×10^{-6} moles) in $CDCl_3$, and (b)-(e) upon addition of 0.5, 2.0, 3.0, 4.0 eq. of **C_{70}** in $CDCl_3$.

***p*-(PTZ)$_4$-H$_2$P**

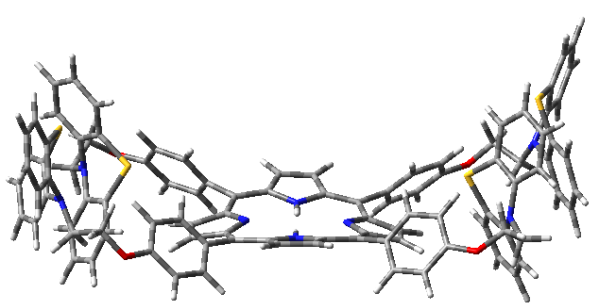

(a)

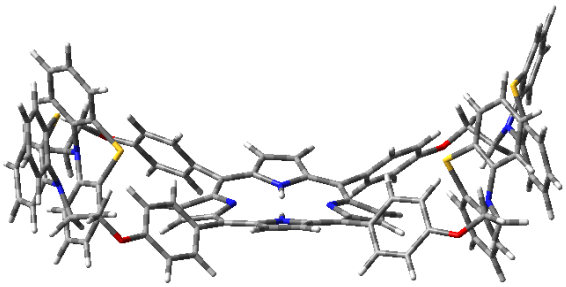

(b)

***m*-(PTZ)$_4$-H$_2$P**

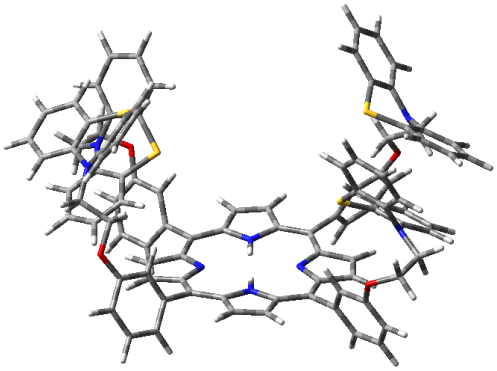

(c)

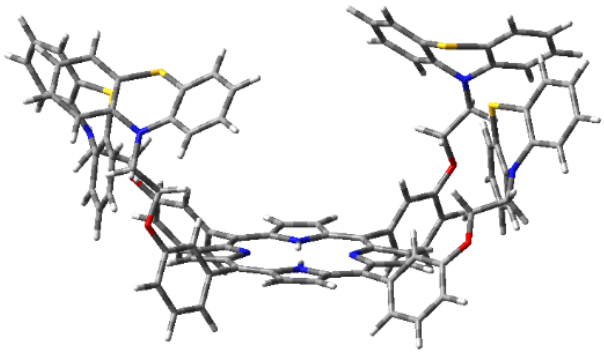

(d)

Fig. S37. B3LYP-D3/6-31G(d) calculated structures of the free porphyrin receptors, ***p*-(PTZ)$_4$-H$_2$P** (a & b) and ***m*-(PTZ)$_4$-H$_2$P** (c & d) optimized to bind **C$_{60}$** and **C$_{70}$** respectively.

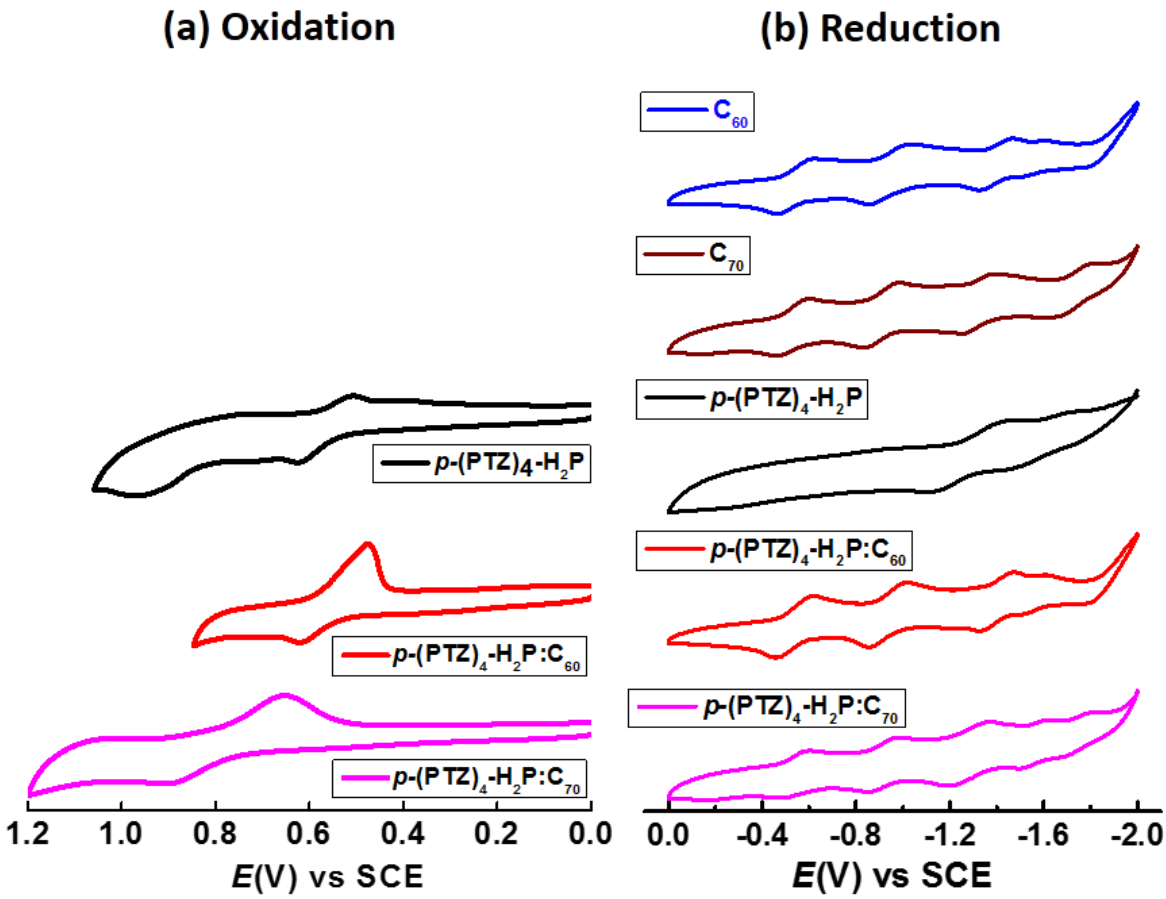

Fig. S38. Cyclic voltammograms of (a) oxidation and (b) reduction of the indicated compounds in 1,2-DCB containing 0.1 M (n-$C_4H_9)_4NClO_4$. The concentrations of the compounds were held at ~ 1 mM; scan rate = 100 mVs^{-1}.

Supporting Information

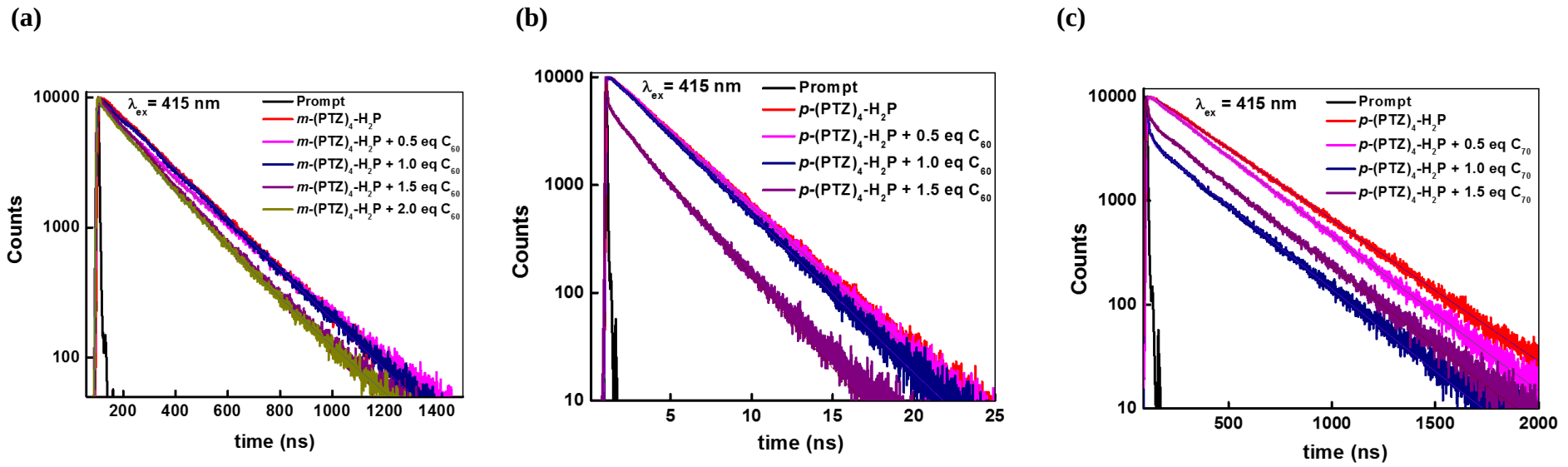

Fig. S39. Fluorescence decay curves of (a) ***m*-(PTZ)$_4$-H$_2$P**in absence and presence of 0.5 – 2.0 eq. of **C$_{60}$**, and ***p*-(PTZ)$_4$-H$_2$P** in presence and absence of (b) 0.5 – 1.5 eq. of **C$_{60}$** and (c) 0.5 – 1.5 eq. of **C$_{70}$**, λ_{ex} = 405 nm in PhCN.

Supporting Information

References:

1. N. Duvva, K. Sudhakar, D. Badgurjar, R. Chitta and L. Giribabu, , *J. Photochem. and Photobiol. A: Chem.* **2015**, *312*, 8-19.
2. A. W. Franz, Z. Zhou, R. Turdean, A. Wagener, B. Sarkar, M. Hartmann, S. Ernst, W. R. Thiel and T. J. Müller, *Eur. J. Org. Chem.*, **2009**, *2009*, 3895-3905.
3. F. A. Walker, *J. Magn. Reson.*, **1974**, *15*, 201-218.
4. C. Lee, W. Yang and R. G. Parr, *Phy. Rev. B.*, **1988**, *37*, 785.
5. W. Kohn, A. D. Becke and R. G. Parr, *The J. Phy. Chem.*, **1996**, *100*, 12974-12980.
6. M. E. Zandler and F. D'Souza, *C R Chim*, **2006**, *9*, 960-981.
7. S. GRIMME and J. ANTONY, *The J. Chem. Phys.*, **2010**, *132*.
8. S. Grimme, S. Ehrlich and L. Goerigk, *J. Comput. Chem.,* **2011**, *32*, 1456-1465.
9. M. Frisch, G. Trucks, H. Schlegel, G. Scuseria, M. Robb, J. Cheeseman, G. Scalmani, V. Barone, G. Petersson and H. Nakatsuji, *Inc., Wallingford CT*, **2016**.